JCI insight

Intranasal Immunization with Peptide-based Immunogenic Complex Enhances BCG Vaccine Efficacy in murine model of Tuberculosis

Santosh Kumar, … , Gobardhan Das, Ved Prakash Dwivedi

JCI Insight. 2021. https://doi.org/10.1172/jci.insight.145228.

Research In-Press Preview **Immunology** **Infectious disease**

Novel prime-boost immunization strategies are required to control the global Tuberculosis (TB) pandemic, which claims approximately 3 lives every minute. Here, we have generated an immunogenic complex against *Mycobacterium tuberculosis* (*M.tb),* consisting of promiscuous T cell epitopes (*M.tb* peptides) and TLR ligands assembled in liposomes. Interestingly, this complex (PTLs; peptide-TLR agonist-liposomes) induced significant activation of $CD4^+$ T cells and IFNγ production in the PBMCs derived from PPD^+ healthy individuals as compared to PPD^- controls. Furthermore, intranasal delivery of PTLs significantly reduced the bacterial burden in the infected mice by inducing *M.tb* specific polyfunctional ($IFN\gamma^+IL17^+TNF\alpha^+IL2^+$) immune responses and long-lasting central memory responses thereby reducing the risk of TB recurrence in DOTS treated infected animals. The transcriptome analysis of peptide-stimulated immune cells unveiled the molecular basis of enhanced protection. Furthermore, PTLs immunization significantly boosted the BCG-primed immune responses against TB. The greatly enhanced efficacy of BCG-PTLs vaccine model in controlling pulmonary TB projects PTLs as an adjunct vaccine against TB.

Intranasal Immunization with Peptide-based Immunogenic Complex Enhances BCG Vaccine Efficacy in murine model of Tuberculosis

Santosh Kumar[1,#], Ashima Bhaskar[2,#], Gautam Patnaik[3], Chetan Sharma[1], Dhiraj Kumar Singh[3, 4], Sandeep Rai Kaushik[1], Shivam Chaturvedi[1], Gobardhan Das[3], Ved Prakash Dwivedi[1,*]

1. International Centre for Genetic Engineering and Biotechnology, New Delhi, India
2. Signal Transduction Laboratory-1, National Institute of Immunology, New Delhi, India
3. Special Center for Molecular Medicine, Jawaharlal Nehru University, New Delhi, India
4. Current Address: Southwest National Primate Research Center, Texas Biomedical Research Institute, San Antonio, TX 78227, USA.

[#] Equal Contribution

*Address for Correspondence

Dr Ved Prakash Dwivedi
Immunobiology Group,
International Centre for Genetic Engineering and Biotechnology,
Aruna Asaf Ali Marg,
New Delhi, Pin Code: 110067,
India
Email: vedprakashbt@gmail.com
Contact No: +91-11-26741358

Running Title: A peptide based vaccine against TB

Keywords: *Mycobacterium tuberculosis*, Vaccine, T helper Cells, BCG, Peptides, Cytokines, Memory Cells

Conflict of Interest: The authors declare that there is no competing interest.

Abstract:

Novel prime-boost immunization strategies are required to control the global Tuberculosis (TB) pandemic, which claims approximately 3 lives every minute. Here, we have generated an immunogenic complex against *Mycobacterium tuberculosis* (*M.tb*), consisting of promiscuous T cell epitopes (*M.tb* peptides) and TLR ligands assembled in liposomes. Interestingly, this complex (PTLs; peptide-TLR agonist-liposomes) induced significant activation of $CD4^+$ T cells and IFNγ production in the PBMCs derived from PPD^+ healthy individuals as compared to PPD^- controls. Furthermore, intranasal delivery of PTLs significantly reduced the bacterial burden in the infected mice by inducing *M.tb* specific polyfunctional ($IFN\gamma^+IL17^+TNF\alpha^+IL2^+$) immune responses and long-lasting central memory responses thereby reducing the risk of TB recurrence in DOTS treated infected animals. The transcriptome analysis of peptide-stimulated immune cells unveiled the molecular basis of enhanced protection. Furthermore, PTLs immunization significantly boosted the BCG-primed immune responses against TB. The greatly enhanced efficacy of BCG-PTLs vaccine model in controlling pulmonary TB projects PTLs as an adjunct vaccine against TB.

Introduction:

Mycobacterium tuberculosis (*M.tb*), the causative agent of tuberculosis (TB) affects about one-fourth of the global population (1). Approximately 2 million deaths globally are directly attributed to TB. Synergism between Human Immunodeficiency Virus (HIV) infections and *M.tb* along with the emergence of multidrug-resistant strains of *M.tb* has become a major concern for nations globally (2, 3). Unfortunately, cost-effective and user-friendly therapy for TB infections is long overdue. *M.tb* infections may produce varied responses between the individuals, ranging from asymptomatic infections to progressive pulmonary or extra-pulmonary TB and even death (4). The rate of progression in the severity of TB depends on the status of the host immune system.

Although world's only accepted vaccine against TB, the live attenuated strains of *Mycobacterium bovis* Bacillus Calmette-Guerin (BCG) is very effective against disseminated and meningeal TB in young children. However, its efficacy in protecting against adult pulmonary TB varies dramatically from 0-80% in different populations depending upon ethnicity and geographical regions (5-9). BCG's limited vaccine efficacy is majorly attributed to its failure to induce a significant population of central memory T cells (T_{CM}) (6, 9-11) as animal models vaccinated with BCG primarily develop antigen-specific $CD4^+$ effector memory T cells (T_{EM}). Considering the lags in BCG immunization and increased global TB

burden, it is crucial to develop improved methods of immuno-prophylaxis against TB. Since, most of the world's population is vaccinated with BCG, we need an alternative therapy to improve the efficacy of BCG in terms of enhancing central memory responses leading to the induction of polyfunctional cytokine responses at the site of infection, eventually controlling the infection.

Surface antigens along with the secretome of mycobacteria have been shown to generate potent host immune responses during *M.tb* infection (12-15). Taking a cue from above findings, in this study we generated an immunogenic complex against *M.tb* which consisted of promiscuous protective T-cell epitopes along with TLR ligands adsorbed on liposomal drug delivery vehicle. These complexes, termed as PTLs (peptide-TLR agonist-liposomes) were delivered directly into the lungs through intranasal route, thereby generating a protective immune response at the site of infection.

We observed that the PTLs significantly enriched the BCG induced T_{CM} pool in the $CD4^+$ and $CD8^+$ T cells with a decrease in the T_{EM} cell pool in the lungs of mice co-immunized with BCG and PTLs as against the mice immunized with BCG or PTLs alone. The population of T_{CM} cells was maintained at elevated numbers in the spleens of co-immunized animals as well, consistent with the understanding that spleens are the potential reservoir of these cells (9). Interestingly, the frequency of immunosuppressive PD-1 expression on memory cell subsets was significantly low in the lungs and spleen of BCG and PTLs co-immunized mice as compared to other groups. Moreover, increased memory responses correlated with a remarkable reduction in bacterial burden in the lungs, spleen, and liver of the animals receiving PTLs immunization along with BCG than in other experimental groups.

Furthermore, we also noticed a significant increase in the polyfunctional cytokine secretion ($IFN\gamma^+IL17^+TNF\alpha^+IL2^+$) in $CD4^+$ and $CD8^+$T cells in the lungs of co-immunized animals as compared to the mice vaccinated with BCG alone. A similar protective response was also observed in reactivation studies. Separate transcriptome analysis of peptide pool pulsed DCs and co-cultured T cells further sheds light on the possible multiple host protective pathways induced by PTLs.

Collectively, in our study, we report that BCG vaccinated mice when co-immunized with PTLs induced a larger pool of T_{CM} cells which may contribute to a stronger and a potent recall immune response to facilitate enhanced *M.tb* clearance. In brief, our findings suggest

that PTLs co-immunization in BCG vaccinated mice significantly enhances the vaccine efficacy of BCG.

Results:

T cell peptides derived from *M.tb* induce host protective immune responses

M.tb peptides derived from ESAT6, Ag85B and MPT70 have been shown to be promising candidates for the induction of protective T cell responses during TB. Taking observation from the previous studies, we screened 14 *M.tb* peptides derived from different secretory proteins of H37Rv, for their efficacy to induce *M.tb* specific T cell activation and host protective Th1/Th17 responses (**Supplementary Table 1**) (12-16). A group of mice infected with H37Rv strain of *M.tb* was subjected to 45 days of DOTS therapy starting from 15 days post-infection. After a rest period of 30 days, T cells from these infected and DOTS treated mice were isolated and co-cultured with dendritic cells (DCs) derived from the bone marrow of naïve mice and pulsed with T cell epitopes/peptides (0.2 μg/ml) or complete soluble antigen (CSA) of *M.tb* (20 μg/ml). From these set of peptides, seven peptides which induced significant T cell activation (**Figure 1A)** and enhanced IFNγ and IL17 secretion **(Figure 1B and 1C)** are indicated in **Supplementary Table 2.** Next, we performed the above experiments using pool of these seven antigenic peptides (combo, 100 ng/ml of each peptide) and CSA of *M.tb* as a positive control. Combo significantly increased the expression of early surface activation marker CD69 on $CD4^+$ cells and $CD8^+$ T cells **(Figure 1D)** in comparison to CSA of *M.tb*. Furthermore, we also observed an increase in the number of IFNγ and IL17 producing $CD4^+$ and $CD8^+$ T cells **(Figure 1E & 1F)** in the T cell pool co-cultured with DCs loaded with peptide pool in comparison to the CSA.

***M.tb* peptides induce gene expression signature required for protective immunity in DCs and T cells**

To further understand the host changes at the transcription levels leading to an increased T cell activation and an augmented pro-inflammatory cytokine upon peptide pool treatment, we performed comparative transcriptome analysis of unstimulated dendritic cells DCs (Un-DC) vs peptide pool pulsed DCs (Pep-DC) and T cells co-cultured with unstimulated DCs (Un-TC) vs T cells co-cultured with peptide pool pulsed DCs (Pep-TC). Our RNAseq data revealed 1452 differentially expressed genes (1098 up-regulated, Log2FC>1 and 354 down-regulated, Log2FC<-1 with FDR $\leq$0.05) in the peptide pool stimulated DCs as compared to unstimulated DCs **(Figure 2A)** while T cells co-cultured with peptide pool pulsed DCs showed 2331 differentially expressed genes (1223 activated and 1108 repressed) as compared

to T cells co-cultured with unstimulated DCs (Accession Number: GSE164258) **(Figure 2B)**. Differential genes in both DCs and T cells after peptide pool stimulation were highly enriched for gene sets assisting in IFNγ response and production, cytokine activity, STAT phosphorylation, ADP metabolic processes, ROS equilibrium, etc **(Supplementary Figure 1A and 1B)**. Many pathways known to play an important role in combatting TB disease were significantly upregulated in peptides stimulated DCs and T cells as indicated by KEGG analysis **(Figure 2C and 2D)**. Differential genes in the DCs as well as the T cells majorly belonged to signaling pathways such as JAK-STAT, Tuberculosis, TNF, TLR and TGFβ signaling **(Figure 2E and 2F)**. The transcriptome data analysis revealed a very similar and indistinguishable trend of activated genes in DCs and T cells. A huge number of 724 genes (586 up-regulated and 138 down-regulated) were common between the two cell types **(Supplementary Figure 1C)**. Moreover, these genes followed the same expression profile in both the settings **(Supplementary Figure 1C)**. KEGG analysis indicated that these genes belonged to a number of TB related protective host signaling pathways such as NFκB, MAPK, TGFβ, TNF, IL17, etc **(Supplementary Figure 1D)**. Taken together, our transcriptomics data strengthened our findings that peptide pool induces an intricate network of signaling pathways in DCs and T cells which leads to enhanced cytokine production and T cell activation.

Induction of immune responses in Human PBMCs by the *M.tb* peptides-TLR agonists-liposome assembly

Subject to above results, we establish here that in combination, our peptides are capable of inducing antigen-specific protective T cells; therefore we assembled these 7 antigenic peptides along with TLR2 and TLR9 agonist Pam3CysSK-4 and CpG ODN respectively, as evidenced by previous reports that TLR2 and TLR9 play an important role during *M.tb* infection (17, 18), in a liposomal delivery vehicle for the successful delivery of this cargo to the lungs through the intranasal route **(Figure 3A).** The efficacy of this assembly of peptides, TLR ligands and liposomes (PTLs) was assessed in human PBMCs derived from 10 PPD^- and 10 PPD^+ BCG vaccinated healthy individuals. The PBMCs were in vitro stimulated with *M.tb* CSA (20 μg/ml), BCG complete soluble antigen (BCG CSA, 20 μg/ml), PTLs (10 μl/ml) and BCG CSA/PTLs for 48h followed by surface/intracellular staining and FACS analysis to determine $CD4^+$ T cell activation and IFNγ production. With no significant difference in PPD^- individuals, PTLs and BCG CSA/PTLs combination induced significant

expression of early activation marker CD69 and IFNγ on $CD4^+$ T cells in the PBMCs derived from PPD^+ individuals as compared to *M.tb* CSA and BCG CSA controls **(Figure 3B-E).**

PTLs immunization following BCG vaccination enhances host protection against TB

To confirm the successful delivery of this assembly of peptides, TLR ligand and liposomes (PTLs) into the lungs, the PTLs were labelled with PKH67 to stain the liposomes (delivery vehicle, see methods) and administered intranasally into the lungs. Two days post-delivery, mice were euthanized and lung sections were prepared for fluorescence microscopy **(Figure 4A)**. Quantification of the fluorescent images indicated the accumulation of liposomes/PTLs throughout the lungs **(Figure 4B).**

Despite its limited efficacy in adults, BCG vaccine is highly successful in young children and as a result, is administered in infants and small children in high burden countries. Keeping in mind the existing load of the global population vaccinated with BCG, we designed a strategy wherein BCG vaccinated mice were boosted with once-a-week, three-week-long PTLs boosting regimen followed by a rest period of 21 days. **Supplementary Figure 2** shows the pre-challenge immune response in the lungs and the spleen of vaccinated animals. With no increase in the number of $CD4^+$ and $CD8^+$ T cells, we observed significant increase in the expression of CD69 on these cells in the lungs of BCG-PTLs co-immunized mice as compared to BCG/PTLs administration alone **(Supplementary Figure 2A-2D)**. Furthermore, co-immunized animals also showed significant increase in the $CD4^+$ T cells expressing IFNγ and IL17 **(Supplementary Figure 2E & 2F)** as compared to single vaccinations. Similarly, $CD8^+$ T cells expressing IL17 but not IFNγ were also induced in the lungs of co-immunized mice **(Supplementary Figure 2G & 2H)**. Similar profile was observed in the spleen of vaccinated animals **(Supplementary Figure 2I–2P)**. These mice were challenged with H37Rv, the laboratory strain of *M.tb* using low dose aerosol infection model (~150 CFU/mice), after which organs were harvested at different time points to look at the bacterial burden along with the elicited immune responses **(Figure 4C)**. Consistent with our expectations, co-immunized animals had fewer and smaller inflammatory lesions in their lungs than mice immunized with BCG or PTLs alone while the non-vaccinated infected mice i.e. primary infection with H37Rv *M.tb* showed a significantly higher number of inflammatory lesions **(Figure 4D)**. These results were further strengthened by histopathological analysis of lungs which confirmed the reduced lung inflammation in the co-immunized group as compared to the rest of the experimental groups **(Figure 4E)**. PTLs co-immunization significantly increased the BCG-induced TB protection, as observed by the

reduced bacterial burden in various organs viz. lungs **(Figure 4F)**, spleens **(Figure 4G)**, and liver **(Figure 4H)** of infected mice. Thus, the PTLs significantly enhanced the anti-tubercular capacity of BCG immunization. Interestingly, the mice immunized with PTLs alone displayed comparable **(Figure 4F)** and enhanced **(Figure 4G and 4H)** resistance against *M.tb* as the BCG immunized group.

BCG-PTLs co-immunization elevates the adaptive immunity in the lungs and the spleen *M.tb* infected mice

The host immune system plays a pivotal role in defending against TB pathogenesis. To delve into the immunological changes involved in enhanced protection conferred by BCG-PTLs co-immunization, we profiled the immune cells in the lungs and the spleen of infected animals. **Figure 5A** describes the gating strategy employed to quantify the percentage of various T cell subsets in the lungs and spleen of infected mice. BCG-PTLs co-immunized mice showed comparable levels and activation of $CD4^+$ **(Figure 5B-D)** whereas with minimal effect on the percentage of $CD8^+$ T cells **(Figure 5E)**, BCG-PTLs co-immunization significantly enhanced the expression of early and late activation markers (CD69 and CD25 respectively) on $CD8^+$ T cells as compared to either BCG or PTLs immunization **(Figure 5F and 5G)**. Further, we observed increased frequency of $CD4^+$ T cells **(Figure 5H)** with increased expression of late activation marker CD25 in the spleen of BCG-PTLs co-immunized animals **(Figure 5I)**. CD69 expression was significantly high in splenic $CD4^+$ T cells derived from PTL immunized immunized animals as compared to BCG group **(Figure 5J)**. Percentage of $CD8^+$ T cells was significantly high in the spleen of BCG-PTLs immunized animals **(Figure 5K)** with no increase in the early and late activation markers **(Figure 5L and 5M)**.

BCG-PTLs co-immunization induces polyfunctional cytokine responses in the lungs and the spleen of *M.tb* infected mice

To investigate the T cell specific cytokine responses in different experimental groups, we isolated the T cells from the lungs and the spleen of treated and control mice and estimated intracellular cytokine production. Polyfunctional T cells expressing more than two cytokines such as IFNγ, TNFα, IL17 and IL2 have been linked with enhanced protection against TB (19, 20). Moreover, the occurrence of these multi-functional T cell is highly important in the context of effective vaccines against various viruses and intracellular bacterial pathogens (21). Thus we analysed the presence of polyfunctional cells in different T cell subsets in the lungs and the spleen of all animal groups **(Figure 6A)**. Interestingly, BCG-PTLs co-immunization significantly increased the frequency of $CD4^+$ and $CD8^+$ T cells expressing

single, double, triple and quadruple cytokines with a concomitant decrease in the T cell population expressing none of the four cytokines in the infected lungs **(Figure 6B and 6C)** and the spleen **(Figure 6D and 6E)** as compared to other groups. Particularly, there was an increased occurrence of 4^+ ($IFN\gamma^+TNF\alpha^+IL17^+IL2^+$), 3^+ ($IFN\gamma^+TNF\alpha^+IL17^+$) and 2^+ ($IF\gamma^+IL17^+$;$TNF\alpha^+IL17^+$) $CD4^+$ and $CD8^+$ T cells in the co-immunized group as compared to other animals **(Figure 6F and 6G)**. However, the expression of single cytokines ($IFN\gamma^+$ & $IL17^+$) was higher only in $CD4^+$ T cells **(Figure 6F and 6G)**. A similar profile was observed in the spleen of co-immunized mice where 4^+ ($IFN\gamma^+TNF\alpha^+IL17^+IL2^+$), 3^+ ($IFN\gamma^+TNF\alpha^+IL17^+$;$IFN\gamma^+TNF\alpha^+IL2^+$), 2^+ ($IFN\gamma^+IL17^+$) and 1^+ ($IFN\gamma^+$) $CD4^+$ and $CD8^+$ T cells displayed significantly enhanced frequency in BCG-PTLs co-immunized group **(Figure 6H and 6I)**. Taken together, we observed that BCG vaccination followed by PTLs immunization greatly enhanced the antigen-specific Th1 and Th17 responses as well as pro-inflammatory cytokines, TNFα and IL2. All these cytokines have been well documented to impart protection against TB.

PTLs immunization induces central memory T cell responses critical for long lasting protection

Since recall responses are mediated by T_{CM}, these cell subtypes become a prerequisite for enhanced vaccine efficacy and superior TB protection (6, 9, 22). Thus we analysed the memory cell profile of the lung as well as the splenic T cell subsets **(Figure 7A)**. We observed that BCG-PTLs co-immunization enriched the vaccine-induced T_{CM} ($CD44^{HI}CCR7^{HI}CD62L^{HI}$) cell pool in $CD4^+$ T cells **(Figure 7B)** with a concomitant decrease in the T_{EM} ($CD44^{HI}CCR7^{LO}CD62L^{LO}$) cell pool **(Figure 7C)** in the lungs of infected mice as compared to BCG vaccinated animals. Expression of inhibitory receptors such as PD-1 and CTLA-4 is often linked with negative regulation and inhibition of activated T cells leading to T cell exhaustion (23, 24). Moreover, in non-human primates and in several human studies, increased PD-1 expression is linked with severe TB pathology and enhanced bacillary load (25, 26). Interestingly, decreased expression of PD-1 was observed on the $CD4^+$ T_{CM} and T_{EM} subsets in the lungs of mice co-immunized with BCG and PTLs as compared to BCG vaccinated group **(Figure 7D and 7E)**. A similar pattern was observed in the $CD8^+$ lung T cells **(Figure 7F-7I)** When investigated in the spleen of co-immunized animals, there was increased frequency of $CD4^+$ T_{CM} pool **(Figure 7I)** with a decrease in $CD4^+$ T_{EM} subset **(Figure 7J).** PD-1 expression was significantly less only in case of $CD4^+$ T_{CM} subset **(Figure 7L)** in the co-immunized group with no effect on $CD4^+$ T_{EM} subset

(Figure 7M). $CD8^+$ T_{CM}/T_{EM} cells were comparable in all the groups **(Figure 7N and 7O).** With no decrease in PD-1 expression on $CD8^+$ T_{CM} **(Figure 7P),** its expression was significantly less on $CD8^+$ T_{EM} subset in the co-immunized group **(Figure 7Q)**. Previously it has been shown that BCG vaccinated or *M.tb*-infected mice generate a profoundly expanded population of antigen-specific T_{EM} cells within the lungs whereas the T_{CM} pool is substantially smaller. However, T_{CM} is maintained in significantly larger numbers in the spleen, which is believed to be a potential reservoir for these cells (9, 22). While we found similar T_{CM}/T_{EM} profiles for infected and BCG-vaccinated controls, co-immunized mice maintained an increased pool of T_{CM} cells both in the spleen and the lungs. Nuclear FOXO1 is in an un-phosphorylated state and keeps the long-lived memory T cells enriched while the phosphorylated FOXO1 protein leaves the nucleus and is tagged for ubiquitin mediated protein degradation (27, 28). Interestingly, we also observed a significant reduction in the phosphorylation of FOXO1 transcription factor in the splenocytes of co-immunized animals in comparison to all other experimental groups **(Supplementary Figure 3)**. We also observed an increased activation of NFkB transcription factor in the splenocytes of BCG-PTLs co-immunized animals as compared to other groups **(Supplementary Figure 3)**. NFkB is believed to be the main transcription factor responsible for the expression of various pro-inflammatory cytokines such as IFNγ, TNFα, IL12, etc required for providing resistance to TB. Collectively, these data suggest that PTLs used in this study induces the activation of key transcription factors involved in generating protective immune responses inside the host.

Antigen-specific protective immunity induced by BCG-PTLs co-immunization can be adoptively transferred by T cells

Above results clearly demonstrate that PTLs co-immunization enhanced protective immune responses following BCG vaccination. To further reveal the antigen specificity and protective function of T cell responses generated by BCG-PTLs co-immunization, we carried out the adoptive transfer of $CD4^+$ and $CD8^+$ T cells isolated from the lungs of BCG, PTLs and BCG-PTLs co-immunized mice to check for their antigenic specific protective response in naïve mice. $CD4^+$ ($1x10^6$) and $CD8^+$ T cells ($1x10^6$) were transferred into gamma irradiated Thy1.1 mice followed by a low-dose aerosol challenge of *M.tb* H37Rv. 25 days post infection, mice were sacrificed for CFU enumeration and immune profiling **(Figure 8A)**. Fairly, we found significant decrease of bacterial load in the mice which received T cells from BCG-PTLs co-immunized animals as compared to BCG vaccinated group **(Figure 8B and 8C)**. Furthermore, the immune profiling revealed a significant increase in the percentage of INFγ

producing $CD4^+$ and $CD8^+$ T cells with no difference in IL17 producing T cells in the spleen of mice which received T cells from BCG-PTLs immunized animals **(Figure 8D-8G)**. Therefore T lymphocytes ($CD4^+$ and $CD8^+$ T cells) isolated from co-immunized mice successfully transferred the protective immunity against TB in naïve animals.

BCG-PTLs co-immunization protects antibiotic-treated animals against disease recurrence

From the above experiments, it is clear that PTLs co-immunization enhances the BCG induced host protective immunity and selectively induces central memory T-cell responses, which generally results in long-term protection against TB. To further determine the extent of long-term protection induced by PTLs co-immunization, we performed re-activation experiments in the mouse model of TB **(Figure 9A)**. Reactivation rate was calculated as the number of mice re-activated out of the total number of mice in that group. The re-activation results showed that non-vaccinated mice receiving INH and RIF treatment exhibited greater disease re-activation (7 mice out of 10, 70%) upon dexamethasone treatment while mice immunized with BCG showed around 40 % (4 mice out of 9) relapse **(Table 1)**. The relapse rate was significantly lower in mice co-immunized with BCG and PTLs (2 mice out of 10, 20%) **(Table 1)**. However, there were no differences in terms of bacterial burden in the mice which experienced re-activation **(Figure 9B)**. Since effective memory equates to enhanced protection from primary as well as secondary infections, these observations demonstrate that enhanced pro-inflammatory responses and T_{CM} responses induced by BCG-PTLs co-immunization might translate into reduced relapse incidents due to re-activation thus effectively promoting sterile immunity.

Discussion:

The ability of host immune response to mount an activated antigenic T cell response in the case of pathogenic insult is must to decrease the pathology associated with the infection. While the knowledge about the exact kind of immune responses mounted by the host in the case of TB is still expanding, the role of IFNγ producing Th1 has been well documented(29-32). Recent work by several labs including ours has shown a synergistic role of Th1 and Th17 cells in mounting potent protective responses against TB (8, 33, 34). The mycobacterial secretory proteins play a crucial role in the induction of protective immune responses during TB infections. Mycobacterial proteins like MPT70, Ag85B and ESAT6 have already been used as candidates for antigenic vaccines against TB (14, 35, 36). Their success in T cell proliferation along with IFNγ assays have made them promising candidates to be considered

in the race for novel sub-unit vaccines against TB owing to their promiscuous nature (14, 35, 36). We screened several *M.tb* antigenic peptides for their ability to induce IFNγ and IL17 and narrowed down to 7 overlapping peptides from Ag85B and ESAT6 **(Figure 1)**. The evidences gathered over a period of time indicates the inability of BCG vaccine in inducing an optimal T cell response against several T cell epitopes harbouring immunogenic antigens (37). Also, the BCG vaccine is rendered relatively ineffective in cases of adult pulmonary TB due to its inability to evoke an optimum protective T cell response in the lungs (the primary site of infection) since peripheral T cells have limited influence in the lungs (37). Thus, our rationale was to improve the vaccine's immunogenic repertoire by including relevant fragments of *M.tb* antigens which might generate an improved response vaccine against TB.

Conventionally *M.tb* produces an array of PAMPs, including lipoarabinomanan, phenolic glycolipids, phosphatidylinositol mannosidase and other lipoproteins. These molecular patterns are recognised by Toll-like receptors (TLRs). TLRs are innate cytosolic surveillance sensors found on professional antigen presenting cells (APCs) such as macrophages and DCs (18, 38). Interestingly, ligation of these PAMPs is known to trigger both protective as well as pathogenic immune responses (18, 38). Moreover, mice lacking MyD88, a major adaptor molecule required for downstream signalling events by the majority of TLR/IL1R family members, demonstrate enhanced susceptibility to aerosol infection with *Mtb* (39). Several groups have provided convincing reports that TLR2 and TLR9 both are indispensable in protection against TB (17, 40-42). Engagement of these TLRs leads to the activation of a spectrum of transcription factors that induce several pro-inflammatory cytokines including IFNγ, which confers protective immunity against TB. Therefore, we included PamCysSK-4 as TLR2 and CpG ODN as TLR9 agonist in our vaccine design. These TLR agonists along with the pool of 7 overlapping *M.tb* peptides were packaged in the liposomes for intranasal delivery into the lungs **(Figure 4A)**.. Impressively, co-immunisation of BCG and PTLs not only reduced the bacterial burden **(Figure 4)** but also led to the increase in the percentage of $CD4^+$ and $CD8^+$ T cells **(Figure 5)** that actively participate in providing protective immunity against TB. We also observed enhanced activation of these T cell subsets. In this study, we have analysed the expression of CD69 and CD25 as early and late T cell activation markers. However, $CD25^+$ T cells expressing Foxp3 represent Treg cells that have an inhibitory role in the T cell activation. This warrants the analysis of other T cell activation markers. In our study, we also observed a significant increase in the percentage of polyfunctional $CD4^+$ and $CD8^+$ T cells producing more than two cytokines in the mice co-immunized with BCG and

PTLs **(Figure 6)**. Moreover, our study also provides strong evidence in favour of antigen-specific nature of these responses from adoptive transfer experiments, where T cells from co-immunized mice were able to impart protective immunity to congenic TB unexposed naïve mice upon *M.tb* infection **(Figure 8)**.

T_{CM} cells, the perpetual source of T_{EM} cells, dictate the recall responses and are considered indispensable towards potent vaccine response providing long lasting protective immunity (22, 43). Recently, superior host protection by ΔureC::hly BCG strains has been attributed to its induction of an enhanced T_{CM} response (11). Interestingly, central memory cells were found to be elevated during co-immunization of PTLs along with BCG **(Figure 7)**. FOXO1 plays an important role in establishing long-lived T cell memory responses. BCG-PTLs co-immunization reduced the phosphorylation of FOXO1 in the splenocytes of infected animals, which leads to its increased localization in the nucleus, thereby enriching the protective T cell memory responses responsible for enhanced efficacy of vaccine (27, 28). Furthermore, the increase in NFκB activation in the co-immunized group corroborated with studies crediting NFκB activation in inducing pro-inflammatory cytokine production during TB **(Supplementary Figure 3)** (44-46).

Transcriptome studies on peptide pool pulsed DCs and stimulated T cells revealed that peptide pool induces differential expression of genes belonging majorly to the immune-relevant signaling pathways such as, JAKSTAT, TNF, TLR, NFκB, MAPK and TGFβ. JAK-STAT pathway is well known to regulate T cell polarization and deregulation of JAK-STAT pathway leads to increased susceptibility during TB (47, 48). Similarly, loss of TNF signaling causes increased mortality due to increased bacterial burden and necrotic death of overladen macrophages and granuloma breakdown (49, 50). Moreover, patients receiving TNF neutralizing therapy have an increased rate of reactivation of latent TB (51). NFkB has been shown to be critical for the expression of many proinflammatory cytokines required for the protection against tuberculosis (45, 52) as NFkB knockout mice succumb to *M.tb* infection (45, 53). Our data also indicated that peptide pool induces MAPK signaling pathways which have a phenomenal role during TB (54). Dephosphorylation of MAPK, ERK and P38 leads to increased susceptibility during tuberculosis (55). There are many reports suggesting that MAPK pathway is not only involved in many aspects of immune responses from initiation of innate immunity to adaptive immunity but also its termination through apoptosis and maintenance of T cell homeostasis (56-58). Moreover, MAPKs phosphorylate and activate downstream molecules, resulting in T cell activation, proliferation, and differentiation into T

helper phenotypes. *M.tb*-induced production of proinflammatory cytokines also depends on MAPK activation (57, 58).

In spite of the limited ability of the BCG vaccine to provide protective immunity against adult pulmonary TB, it is quite effective in mounting a strong protective response in young children against meningeal and other disseminated TB. Considering that a large percentage of the population in countries with high TB burden are BCG vaccinated at birth, an improvised strategy like ours that accentuates BCG efficacy by selectively increasing central memory T cell pools and polyfunctional T cells which in turn provide long-lasting immune response against TB is long desired. The study warrants further validation in TB models more close to humans such as non-human primates.

Materials and Methods:Mice

All C57BL/6 mice (6–8 wks of age) were maintained in the animal facility of the International Centre for Genetic Engineering and Biotechnology (ICGEB), New Delhi, India and provided for experiments as and when required.

Generation of DCs

C57BL/6 Mice were euthanized, and the femurs were isolated. Bone marrow was flushed out with RPMI 1640 medium using a 2.0-ml syringe (26.5 gauge). The cells were washed twice with PBS and then cultured in complete RPMI 1640 medium (Gibco, In-vitrogen, UK) supplemented with GMCSF (40 ng/ml) and IL4 (10 ng/ml) on 12-well plates (one million cells/ml). On the 3rd day, 75% of the medium was replaced with fresh DC culture medium. On day 5^{th}, the suspended cells were removed, and the loosely adherent cells were collected as immature DCs (CD11c- positive cells were >90%). For mature DCs, immature DCs were stimulated with lipopolysaccharide (LPS, 1 μg/ml) for 24 h. FACS analysis using anti-CD11c, -CD80, -CD86, and -MHC class II antibodies suggested that >90% of the cells were conventional DCs. DCs were either left untreated or treated overnight with 20 μg/ml of CSA or 0.2 μg/ml of each peptide followed by co-culture with $CD3^+$ T cells isolated from *M.tb* infected and DOTS treated animals for 48h.

Human Peripheral Blood Mononuclear Cell (PBMC) isolation

Blood samples collected from PPD^- and PPD^+ BCG vaccinated healthy individuals were diluted in DPBS (Gibco, 14190250) at a ratio 1:2 and layered onto Ficoll-PaqueTMPlus (Cat. No. GE17-1440-02) followed by centrifugation at 500g for 35 minutes. Out of the four layers, the uppermost plasma was removed by pipette and second layer of the cells containing PBMCs were gently removed and suspended in complete DMEM medium (Gibco, In-

vitrogen, UK). These cells were then pelleted, counted and seeded in the 12 well plates for further experiments.

_M.tb_ infection of mice and estimation of Colony Forming Units (CFU)

Mycobacterium tuberculosis H37Rv and BCG cultures were grown in 7H9 (Middlebrooks, Difco™, USA) medium supplemented with 10% OADC (oleic acid, albumin, dextrose, and catalase; Difco™, USA) and with 0.05% Tween 80 and 0.5% glycerol, and cultures were grown to mid-log phase. Aliquots of the cultures in 20% glycerol were preserved at -80^{o}C and these cryopreserved stocks were used for infections.

Mice were infected with H37Rv via the aerosol route using a Madison aerosol chamber (University of Wisconsin, Madison, WI) with its nebulizer pre-calibrated to deposit around of 150 bacilli to the lungs of each mouse as previously described (8). Briefly, bacterial stocks were recovered from freezer and quickly thawed and subjected to light ultra-sonication to obtain a single cell suspension. 15 ml of the bacterial cell suspension (10×10^{6} cells per ml) was placed in the nebulizer of the Madison aerosol chamber pre-calibrated to deliver the desired number of CFUs to the lungs of animals placed inside the chamber, via the aerosol route. At day one post infection, three randomly selected mice were sacrificed and lungs were harvested, homogenized in 0.2 μm filtered PBS and neat samples (without any dilution) plated onto 7H11 Middlebrooks (Difco USA) plates containing 10% oleic acid, albumin, dextrose and catalase (OADC) (Difco, USA). Neat, ten-fold diluted and one hundred-fold diluted lung, liver and spleen cells homogenates were plated in triplicate on the 7H11 plates and incubated at 37°C for 21-28 days for the organs harvested at different time points. Colonies were counted and CFU was calculated accordingly. Mice from various groups were euthanized at the indicated time points in various experiments; their organs were harvested for obtaining CFU counts and/or immune cell subpopulations for immunological studies as described under other sub-sections.

Antibiotic treatment

Thirty days post infection; groups of mice were treated with 10mg/kg of rifampicin and 10mg/kg of isoniazid (Sigma-Aldrich, St. Louis, MO, USA) administered in the drinking water (changed daily) for 12 weeks. *M.tb* infected control mice received plain drinking water.

Isolation of T cell lymphocytes from _M.tb_ infected animals

Lungs and spleen from infected animals were harvested and washed by swirling in PBS. They were opened up by cutting longitudinally and then cut into, 0.5 cm pieces. These lung pieces were agitated in 25 ml of extraction buffer (PBS, 3% FCS, 1 mM dithiothreitol, 1 mM

EDTA) for 30 min at 37^{o}C. This slurry was passed through a loosely packed nylon wool column to remove the aggregates. The filtrate was layered on a discontinuous Percoll gradient (Amersham Pharmacia Biotech, USA). This gradient was then centrifuged at 1500rpm for 20 minutes. Cells at the interface were collected and washed in staining buffer (PBS, 3% FCS). Spleen cells were homogenized and washed with RBC lysis buffer to remove RBCs. Cells from the lungs and spleen were cultured for surface and intracellular staining as described in the subsection.

Preparation of PTLs

Lipid mixtures were received from Sigma-Aldrich (Cat No: L4395) were used for the preparation of Liposomes which can encapsulate a broad spectrum of hydrophilic and amphipathic molecules of the low, medium, and high molecular weight (including peptides, proteins, and oligo- and polynucleotides). We mixed the *M.tb* peptides with lipid mixtures along with TLR2 and TLR9 ligands Pam3Cys-SK-4 (Cat: ALX-165-066-M002, Enzo Life Sciences) and CpG ODN (Cat: ALX-746-003-C100, Enzo Life Sciences) respectively as per manufacturer's protocol to get the homogeneous mixture of peptides and TLRligands with liposomes (1 ml of PTLs mixture contains 10 µg of each peptide, 100 µg of Pam3Cys-SK-4 and 10 µg of CpG ODN). Then these mixtures were injected intranasally into the mice (50 µl per mice per dose). To confirm the succesfull delivery of the lipososmes into the lungs, the liposomes were stained with PKH67 dye (Sigma-Aldrich) as per manufacturer's protocol. Sections of the lungs were seen under microscope for the fluorescence of the dye.

Immunization

Mice were immunized with (i) BCG (Subcutâneos; SC) ($1x10^{6}$ bacteria), (ii) PTLs (Intranasal; IN), (iii) BCG (SC) + PTLs (IN) and (iv) vector only. Mice were subsequently rested for 21 days and then challenged with *M.tb* strain H37Rv by the aerosol route. Organs like lungs, livers and spleens were harvested for determination of bacterial burden and profiling of immune memory cell responses at different days post infection.

Histology

Lung tissues were fixed in formalin solution and coated with wax for sectioning. Sections were stained with Hematoxylin and Eosin (H&E) dyes and slides were acquired under a microscope. Granulomas were analyzed to obtain the granuloma score.

Flow Cytometry: surface and intracellular staining

Spleens and lungs were isolated from respective mice and macerated by frosted slides in ice-cold RPMI 1640 (Gibco, Invitrogen, UK) containing 10% FBS to prepare a single cell suspension. Red blood cells (RBCs) were lysed with RBC cell lysis buffer, incubated at room

temperature for 2-3 minutes and washed with RPMI 1640 containing 10% FBS. The cells were counted and 1×10^6 cells were used for surface staining. For intracellular staining 1×10^6 cells were cultured per well in 12 well plates (Tarsons, USA) in the presence of H37Rv Complete Soluble Antigen (CSA) overnight. Subsequently, 0.5 µg/ml Brefeldin A and 0.5 µg/ml of Monensin solution (Biolegend, USA) were added during the last 4 hours of culture. Cells were then washed twice with FACS buffer (PBS+3%FCS) and stained with antibodies directed against surface markers. After staining, cells were washed again with FACS buffer and fixed with 100µl fixation buffer (Biolegend, USA) for 30 minutes, then washed and re-suspended in 200µl permeabilization buffer (Biolegend, USA) and stained with fluorescently labeled anti-cytokine antibodies. FACS Verse BD was used for acquiring the cell population and data analysis was done using Flow Jo (Tree star, USA).

Antibodies and reagents

We used the following Biolegend antibodies: anti-CD3 (clone: 17A2 and HIT3a)-Pacific-blue or -FITC, PE, APC anti-CD4 (clone: GK1.5 and A161A1)-FITC, -PE, -PerCP-Cy5, -PE/Cy7 or -APC, anti-CD8 (clone: 53-6.7)-FITC, -APC/Cy7, or -APC, anti-CD44 (clone: IM7)-FITC, anti-CD62L (clone: MEL-14)-APC, anti-CD25 (clone: 3C7)-APC, anti-CD69 (clone: H1.2F3 and FN50)-FITC, PE, anti-CD197 or CCR7 (clone: 4B12)-PE/Cy7, anti-IFNγ (clone: XMG1.2 and 4S.B3)-APC, PE, anti-IL12 (clone: C15.6)-PerCP/Cy5.5, anti-IL17 (clone: TC11-18H10.1)-PE-Cy-7, anti-IL2 (clone: JES6-5H4)-FITC, anti-TNFα (clone: MP6-XT22)-PE, PerCP/Cy5.5 anti-TGFβ (clone: TW7-16B4)-APC (all from Biolegend, USA). Brefeldin A Solution (1,000X), Monensin Solution (1,000X) (Cat: 420701) and Intracellular Staining Permeabilization Wash Buffer (10X) were purchased from Biolegend, USA.

T cell Adoptive Transfer

For adoptive transfer experiments, T cells from lungs of the infected mice which belonged to three groups: (i) BCG immunized (ii) PTLs immunized and (iii) BCG-PTLs co-immunized were isolated and sorted into $CD4^+$ and $CD8^+$ T cells. $CD4^+$ ($1.0x10^6$ cells/mouse) and $CD8^+$ T cells ($1.0x10^6$ cells/mouse) were adoptively transferred into gamma irradiated Thy1.1 mice Recipient mice were challenged with H37Rv through the aerosol route for the determination of bacterial burden and immune responses in the lungs of respective mice.

Mouse model of TB re-activation

Mice infected with *M.tb,* with low-dose aerosol infection model, were treated with 10mg/kg of INH and RIF administered *ad libitum* (in the drinking water) or treated to mice co-immunized with BCG and PTLs or immunized with BCG alone for 12 weeks starting at 4th week after infection. These mice were then rested for 30 days followed by treatment with

dexamethasone (5 mg/kg administered intraperitoneally) three times per week for 30 days. These mice were again rested for next 30 days. 10 mice from each group were then sacrificed and CFUs were estimated from lung homogenates to determine the reactivation rate of *M.tb*.

RNA Sequencing (Transcriptomics analysis)

Total RNA was isolated from unstimulated Dendritic cells (Un-DC) and DCs pulsed with peptide pool (Pep-DC) as well as from unstimulated co-cultured T cells (Un-TC) and co-cultured T cells (Pep-TC) along with DCs pulsed with peptide pool using an RNeasy RNA isolation kit (Qiagen, USA). The raw reads generated for unstimulated DCs and peptide pool pulsed DCs and unstimulated Co-cultured T cells and T cells co-cultured with peptide pool pulsed DCs were subjected to quality check using Fast QC (version 0.11.5, http://www.bioinformatics.babraham.ac.uk/projects/fastqc/) using the parameters like base quality score distribution, sequence quality score distribution, average base content per read and GC distribution in the reads. Illumina Adapters (AGATCGGAAGAGC) was removed using Trim Galore (version 0.4.1), a wrapper script to automate quality and adapter trimming as well as quality control. Clean reads were mapped on reference Mus-musculus_GRCm38.p6 using TopHat v2.1.0. Differential analysis was performed on counted mapped reads in range of positions on a chromosome for (Un-DC) vs (Pep-DC), and (Un-TC) vs (Pep-TC) combinations, predicted using htseq-count software and then differential gene expression was found using DeSeq, a bio-conductor R package that estimate variance-mean dependence in count data and implements a range of statistical methodology based on the negative binomial distributions. Functional annotation for combination was performed using Uniprot database, and DAVID. The Transcriptome data is available on gene expression omnibus (Accession Number: GSE164258).

Western Blot

Spleen were harvested from all experimental groups and homogenized and made the cell lysate. Whole cell lysate was prepared by using lysis buffer (50 mM Tris-HCl, pH 7.4, 5 mM EDTA, 120 mM NaCl, 0.5% Nonidet P-40, 0.5 mM NaF, 1 mM dithiothreitol, 0.5 mM phenylmethylsulfonyl fluoride) along with HALT^{TM} phosphatase inhibitor mixture (78420; Thermo Scientific) and protease inhibitor mixture (78410; Thermo Scientific) for 1 hour. Samples were electrophoresed on a 10% SDS-polyacrylamide gel and electroblotted onto polyvinylidene difluoride (PVDF) membranes. Blots were blocked for 1 h in 5% BSA in PBST (PBS with 0.1% Tween 20). NFkB, pNFkB, FOXO1 and pFOXO1 proteins were detected with NFkB (8242S), pNFkB (3033S), FOXO1 (2880S) and pFOXO1 (9461S) monoclonal antibodies, respectively, at a dilution of 1:250 and as recommended by the

manufacturer (Cell Signaling Technology, Inc, USA). Goat anti-rabbit immunoglobulin G-conjugated horse- radish peroxidase (Sc-2004) (diluted 1:5000) was used as a secondary antibody (Santa Cruz Biotechnology). Immunoblotting for β-actin was carried out to confirm equal loading.

Statistical analysis

Statistical analyses were conducted using graph pad prism software by performing two-tailed student's t-test or one-way ANOVA followed by multiple tukey tests. A value of $p<0.05$ was accepted as an indication of statistical significance.*$p<0.05$, **$p<0.005$, ***$p<0.0005$.

Study approval:

Animal experiments were performed as per ethical guidelines approved by the Institutional Animal Ethics Committee held in July 2015 at the International Centre for Genetic Engineering and Biotechnology (ICGEB) (New Delhi, India) and the Department of Biotechnology guidelines (Government of India) (Approval ID: ICGEB/AH/2015/01/IMM-45). All mice used for experiments were ethically sacrificed by asphyxiation in carbon dioxide according to the institutional and Department of Biotechnology, Government of India, regulations. The human studies were ethically approved (Approval ID: 359/SHRMU/19/2010/07) by the Institutional Human Ethics Committee, Jawaharlal Nehru University, New Delhi, India and Regional Medical Research Centre (RMRC), Odisha, India.

Acknowledgements:

We acknowledge the support of the DBT-supported Tuberculosis Aerosol Challenge Facility (TACF), at the International Centre for Genetic Engineering and Biotechnology (ICGEB), and Animal House, ICGEB, New Delhi, India, and their staff in accomplishing this work. We would like to acknowledge Dr Ranjan Kumar Nanda, Translational Health Group, ICGEB, New Delhi, India for providing the resources for the study. VPD and AB are the recipient of DST-INSPIRE Faculty Fellowship from Department of Science and Technology, Government of India and VPD is also recipient of Early Career Research Award from Science Engineering Recruitment Board (SERB), Department of Science and Technology, Government of India. We would like to acknowledge the funding support provided by ICGEB, New Delhi, India. The authors declare no competing financial interests.

Author Contribution:

SK and VPD initially started the study. SK, AB, CS, SRK, DKS, SC and VPD performed *in vitro* experiments and analyzed data. SK, AB and VPD performed all animal experiments. SRK also assisted in animal experiments. GP performed experiments with Human PBMCs.

VPD conceived the hypothesis and supervised the experiments. AB and VPD designed experiments and analyzed the data. GD provided the resources and edited the manuscript. AB and VPD wrote the manuscript.

References:

1. WHO. Global Tuberculosis Report 2017.
2. Matteelli A, Roggi A, and Carvalho AC. Extensively drug-resistant tuberculosis: epidemiology and management. *Clinical epidemiology.* 2014;6(111-8.
3. O'Donnell MR, Padayatchi N, Kvasnovsky C, Werner L, Master I, and Horsburgh CR, Jr. Treatment outcomes for extensively drug-resistant tuberculosis and HIV co-infection. *Emerging infectious diseases.* 2013;19(3):416-24.
4. Sharma SK, Mohan A, and Sharma A. Challenges in the diagnosis & treatment of miliary tuberculosis. *The Indian journal of medical research.* 2012;135(5):703-30.
5. Andersen P, and Doherty TM. The success and failure of BCG - implications for a novel tuberculosis vaccine. *Nature reviews Microbiology.* 2005;3(8):656-62.
6. Bhattacharya D, Dwivedi VP, Kumar S, Reddy MC, Van Kaer L, Moodley P, and Das G. Simultaneous inhibition of T helper 2 and T regulatory cell differentiation by small molecules enhances Bacillus Calmette-Guerin vaccine efficacy against tuberculosis. *J Biol Chem.* 2014;289(48):33404-11.
7. Bhattacharya D, Dwivedi VP, Maiga M, Maiga M, Van Kaer L, Bishai WR, and Das G. Small molecule-directed immunotherapy against recurrent infection by Mycobacterium tuberculosis. *The Journal of biological chemistry.* 2014;289(23):16508-15.
8. Chatterjee S, Dwivedi VP, Singh Y, Siddiqui I, Sharma P, Van Kaer L, Chattopadhyay D, and Das G. Early secreted antigen ESAT-6 of Mycobacterium tuberculosis promotes protective T helper 17 cell responses in a toll-like receptor-2-dependent manner. *PLoS Pathog.* 2011;7(11):e1002378.
9. Singh DK, Dwivedi VP, Ranganathan A, Bishai WR, Van Kaer L, and Das G. Blockade of the Kv1.3 K+ Channel Enhances BCG Vaccine Efficacy by Expanding Central Memory T Lymphocytes. *The Journal of infectious diseases.* 2016;214(9):1456-64.
10. Maggioli MF, Palmer MV, Thacker TC, Vordermeier HM, McGill JL, Whelan AO, Larsen MH, Jacobs WR, Jr., and Waters WR. Increased TNFalpha/IFNgamma/IL2 and Decreased TNFalpha/IFNgamma Production by Central Memory T Cells Are Associated with Protective Responses against Bovine Tuberculosis Following BCG Vaccination. *Frontiers in immunology.* 2016;7(421.
11. Vogelzang A, Perdomo C, Zedler U, Kuhlmann S, Hurwitz R, Gengenbacher M, and Kaufmann SH. Central memory CD4+ T cells are responsible for the recombinant Bacillus Calmette-Guerin DeltaureC::hly vaccine's superior protection against tuberculosis. *The Journal of infectious diseases.* 2014;210(12):1928-37.
12. Kruh-Garcia NA, Murray M, Prucha JG, and Dobos KM. Antigen 85 variation across lineages of Mycobacterium tuberculosis-implications for vaccine and biomarker success. *Journal of proteomics.* 2014;97(141-50.
13. Lee BY, and Horwitz MA. T-cell epitope mapping of the three most abundant extracellular proteins of Mycobacterium tuberculosis in outbred guinea pigs. *Infection and immunity.* 1999;67(5):2665-70.
14. Mustafa AS, Shaban FA, Abal AT, Al-Attiyah R, Wiker HG, Lundin KE, Oftung F, and Huygen K. Identification and HLA restriction of naturally derived Th1-cell epitopes from the secreted Mycobacterium tuberculosis antigen 85B recognized by antigen-specific human CD4(+) T-cell lines. *Infection and immunity.* 2000;68(7):3933-40.
15. Panigada M, Sturniolo T, Besozzi G, Boccieri MG, Sinigaglia F, Grassi GG, and Grassi F. Identification of a promiscuous T-cell epitope in Mycobacterium tuberculosis Mce proteins. *Infection and immunity.* 2002;70(1):79-85.

16. Fan X, Gao Q, and Fu R. Differential immunogenicity and protective efficacy of DNA vaccines expressing proteins of Mycobacterium tuberculosis in a mouse model. *Microbiological research.* 2009;164(4):374-82.
17. Bafica A, Scanga CA, Feng CG, Leifer C, Cheever A, and Sher A. TLR9 regulates Th1 responses and cooperates with TLR2 in mediating optimal resistance to Mycobacterium tuberculosis. *The Journal of experimental medicine.* 2005;202(12):1715-24.
18. Drennan MB, Nicolle D, Quesniaux VJ, Jacobs M, Allie N, Mpagi J, Fremond C, Wagner H, Kirschning C, and Ryffel B. Toll-like receptor 2-deficient mice succumb to Mycobacterium tuberculosis infection. *The American journal of pathology.* 2004;164(1):49-57.
19. Day CL, Abrahams DA, Lerumo L, Janse van Rensburg E, Stone L, O'Rie T, Pienaar B, de Kock M, Kaplan G, Mahomed H, et al. Functional capacity of Mycobacterium tuberculosis-specific T cell responses in humans is associated with mycobacterial load. *Journal of immunology.* 2011;187(5):2222-32.
20. Harari A, Rozot V, Bellutti Enders F, Perreau M, Stalder JM, Nicod LP, Cavassini M, Calandra T, Blanchet CL, Jaton K, et al. Dominant TNFalpha+ Mycobacterium tuberculosis-specific CD4+ T cell responses discriminate between latent infection and active disease. *Nature medicine.* 2011;17(3):372-6.
21. Lewinsohn DA, Lewinsohn DM, and Scriba TJ. Polyfunctional CD4(+) T Cells As Targets for Tuberculosis Vaccination. *Frontiers in immunology.* 2017;8(1262.
22. Henao-Tamayo MI, Ordway DJ, Irwin SM, Shang S, Shanley C, and Orme IM. Phenotypic definition of effector and memory T-lymphocyte subsets in mice chronically infected with Mycobacterium tuberculosis. *Clinical and vaccine immunology : CVI.* 2010;17(4):618-25.
23. Wherry EJ. T cell exhaustion. *Nature immunology.* 2011;12(6):492-9.
24. Wherry EJ, and Kurachi M. Molecular and cellular insights into T cell exhaustion. *Nature reviews Immunology.* 2015;15(8):486-99.
25. Day CL, Abrahams DA, Bunjun R, Stone L, de Kock M, Walzl G, Wilkinson RJ, Burgers WA, and Hanekom WA. PD-1 Expression on Mycobacterium tuberculosis-Specific CD4 T Cells Is Associated With Bacterial Load in Human Tuberculosis. *Frontiers in immunology.* 2018;9(1995.
26. Qiu L, Huang D, Chen CY, Wang R, Shen L, Shen Y, Hunt R, Estep J, Haynes BF, Jacobs WR, Jr., et al. Severe tuberculosis induces unbalanced up-regulation of gene networks and overexpression of IL22, MIP-1alpha, CCL27, IP-10, CCR4, CCR5, CXCR3, PD1, PDL2, IL3, IFNbeta, TIM1, and TLR2 but low antigen-specific cellular responses. *The Journal of infectious diseases.* 2008;198(10):1514-9.
27. Carrette F, Fabre S, and Bismuth G. FOXO1, T-cell trafficking and immune responses. *Advances in experimental medicine and biology.* 2009;665(3-16.
28. Nakae J, Kitamura T, Silver DL, and Accili D. The forkhead transcription factor Foxo1 (Fkhr) confers insulin sensitivity onto glucose-6-phosphatase expression. *The Journal of clinical investigation.* 2001;108(9):1359-67.
29. Flynn JL, and Chan J. Immunology of tuberculosis. *Annual review of immunology.* 2001;19(93-129.
30. Sugawara I, Yamada H, and Mizuno S. Relative importance of STAT4 in murine tuberculosis. *Journal of medical microbiology.* 2003;52(Pt 1):29-34.
31. Sweeney KA, Dao DN, Goldberg MF, Hsu T, Venkataswamy MM, Henao-Tamayo M, Ordway D, Sellers RS, Jain P, Chen B, et al. A recombinant Mycobacterium smegmatis induces potent bactericidal immunity against Mycobacterium tuberculosis. *Nature medicine.* 2011;17(10):1261-8.

32. Lienhardt C, Azzurri A, Amedei A, Fielding K, Sillah J, Sow OY, Bah B, Benagiano M, Diallo A, Manetti R, et al. Active tuberculosis in Africa is associated with reduced Th1 and increased Th2 activity in vivo. *European journal of immunology.* 2002;32(6):1605-13.
33. Khader SA, Bell GK, Pearl JE, Fountain JJ, Rangel-Moreno J, Cilley GE, Shen F, Eaton SM, Gaffen SL, Swain SL, et al. IL23 and IL17 in the establishment of protective pulmonary CD4+ T cell responses after vaccination and during Mycobacterium tuberculosis challenge. *Nature immunology.* 2007;8(4):369-77.
34. Khader SA, and Cooper AM. IL23 and IL17 in tuberculosis. *Cytokine.* 2008;41(2):79-83.
35. Al-Attiyah R, Shaban FA, Wiker HG, Oftung F, and Mustafa AS. Synthetic peptides identify promiscuous human Th1 cell epitopes of the secreted mycobacterial antigen MPB70. *Infection and immunity.* 2003;71(4):1953-60.
36. Ravn P, Demissie A, Eguale T, Wondwosson H, Lein D, Amoudy HA, Mustafa AS, Jensen AK, Holm A, Rosenkrands I, et al. Human T cell responses to the ESAT-6 antigen from Mycobacterium tuberculosis. *The Journal of infectious diseases.* 1999;179(3):637-45.
37. Moliva JI, Turner J, and Torrelles JB. Immune Responses to Bacillus Calmette-Guerin Vaccination: Why Do They Fail to Protect against Mycobacterium tuberculosis? *Frontiers in immunology.* 2017;8(407.
38. Means TK, Jones BW, Schromm AB, Shurtleff BA, Smith JA, Keane J, Golenbock DT, Vogel SN, and Fenton MJ. Differential effects of a Toll-like receptor antagonist on Mycobacterium tuberculosis-induced macrophage responses. *Journal of immunology.* 2001;166(6):4074-82.
39. Reiling N, Holscher C, Fehrenbach A, Kroger S, Kirschning CJ, Goyert S, and Ehlers S. Cutting edge: Toll-like receptor (TLR)2- and TLR4-mediated pathogen recognition in resistance to airborne infection with Mycobacterium tuberculosis. *Journal of immunology.* 2002;169(7):3480-4.
40. Ahmad-Nejad P, Hacker H, Rutz M, Bauer S, Vabulas RM, and Wagner H. Bacterial CpG-DNA and lipopolysaccharides activate Toll-like receptors at distinct cellular compartments. *European journal of immunology.* 2002;32(7):1958-68.
41. Latz E, Schoenemeyer A, Visintin A, Fitzgerald KA, Monks BG, Knetter CF, Lien E, Nilsen NJ, Espevik T, and Golenbock DT. TLR9 signals after translocating from the ER to CpG DNA in the lysosome. *Nature immunology.* 2004;5(2):190-8.
42. Underhill DM, Ozinsky A, Smith KD, and Aderem A. Toll-like receptor-2 mediates mycobacteria-induced proinflammatory signaling in macrophages. *Proceedings of the National Academy of Sciences of the United States of America.* 1999;96(25):14459-63.
43. Ahlers JD, and Belyakov IM. Memories that last forever: strategies for optimizing vaccine T-cell memory. *Blood.* 2010;115(9):1678-89.
44. Bai X, Feldman NE, Chmura K, Ovrutsky AR, Su WL, Griffin L, Pyeon D, McGibney MT, Strand MJ, Numata M, et al. Inhibition of nuclear factor-kappa B activation decreases survival of Mycobacterium tuberculosis in human macrophages. *PloS one.* 2013;8(4):e61925.
45. Fallahi-Sichani M, Kirschner DE, and Linderman JJ. NFkappaB Signaling Dynamics Play a Key Role in Infection Control in Tuberculosis. *Frontiers in physiology.* 2012;3(170.
46. Tchou-Wong KM, Tanabe O, Chi C, Yie TA, and Rom WN. Activation of NFkappaB in Mycobacterium tuberculosis- induced interleukin-2 receptor expression in

mononuclear phagocytes. *American journal of respiratory and critical care medicine.* 1999;159(4 Pt 1):1323-9.
47. Manca C, Tsenova L, Freeman S, Barczak AK, Tovey M, Murray PJ, Barry C, and Kaplan G. Hypervirulent M. tuberculosis W/Beijing strains upregulate type I IFNs and increase expression of negative regulators of the Jak-Stat pathway. *Journal of interferon & cytokine research : the official journal of the International Society for Interferon and Cytokine Research.* 2005;25(11):694-701.
48. Seif F, Khoshmirsafa M, Aazami H, Mohsenzadegan M, Sedighi G, and Bahar M. The role of JAK-STAT signaling pathway and its regulators in the fate of T helper cells. *Cell communication and signaling : CCS.* 2017;15(1):23.
49. Lin PL, Myers A, Smith L, Bigbee C, Bigbee M, Fuhrman C, Grieser H, Chiosea I, Voitenek NN, Capuano SV, et al. Tumor necrosis factor neutralization results in disseminated disease in acute and latent Mycobacterium tuberculosis infection with normal granuloma structure in a cynomolgus macaque model. *Arthritis and rheumatism.* 2010;62(2):340-50.
50. Lin PL, Pawar S, Myers A, Pegu A, Fuhrman C, Reinhart TA, Capuano SV, Klein E, and Flynn JL. Early events in Mycobacterium tuberculosis infection in cynomolgus macaques. *Infection and immunity.* 2006;74(7):3790-803.
51. Marino S, Sud D, Plessner H, Lin PL, Chan J, Flynn JL, and Kirschner DE. Differences in reactivation of tuberculosis induced from anti-TNF treatments are based on bioavailability in granulomatous tissue. *PLoS computational biology.* 2007;3(10):1909-24.
52. Caamano J, and Hunter CA. NFkappaB family of transcription factors: central regulators of innate and adaptive immune functions. *Clinical microbiology reviews.* 2002;15(3):414-29.
53. Yamada H, Mizuno S, Reza-Gholizadeh M, and Sugawara I. Relative importance of NFkappaB p50 in mycobacterial infection. *Infection and immunity.* 2001;69(11):7100-5.
54. Schorey JS, and Cooper AM. Macrophage signalling upon mycobacterial infection: the MAP kinases lead the way. *Cellular microbiology.* 2003;5(3):133-42.
55. Blumenthal A, Ehlers S, Ernst M, Flad HD, and Reiling N. Control of mycobacterial replication in human macrophages: roles of extracellular signal-regulated kinases 1 and 2 and p38 mitogen-activated protein kinase pathways. *Infection and immunity.* 2002;70(9):4961-7.
56. Adler HS, Kubsch S, Graulich E, Ludwig S, Knop J, and Steinbrink K. Activation of MAP kinase p38 is critical for the cell-cycle-controlled suppressor function of regulatory T cells. *Blood.* 2007;109(10):4351-9.
57. Dong C, Davis RJ, and Flavell RA. MAP kinases in the immune response. *Annual review of immunology.* 2002;20(55-72.
58. Pasquinelli V, Rovetta AI, Alvarez IB, Jurado JO, Musella RM, Palmero DJ, Malbran A, Samten B, Barnes PF, and Garcia VE. Phosphorylation of mitogen-activated protein kinases contributes to interferon gamma production in response to Mycobacterium tuberculosis. *The Journal of infectious diseases.* 2013;207(2):340-50.

Figures and Legends:

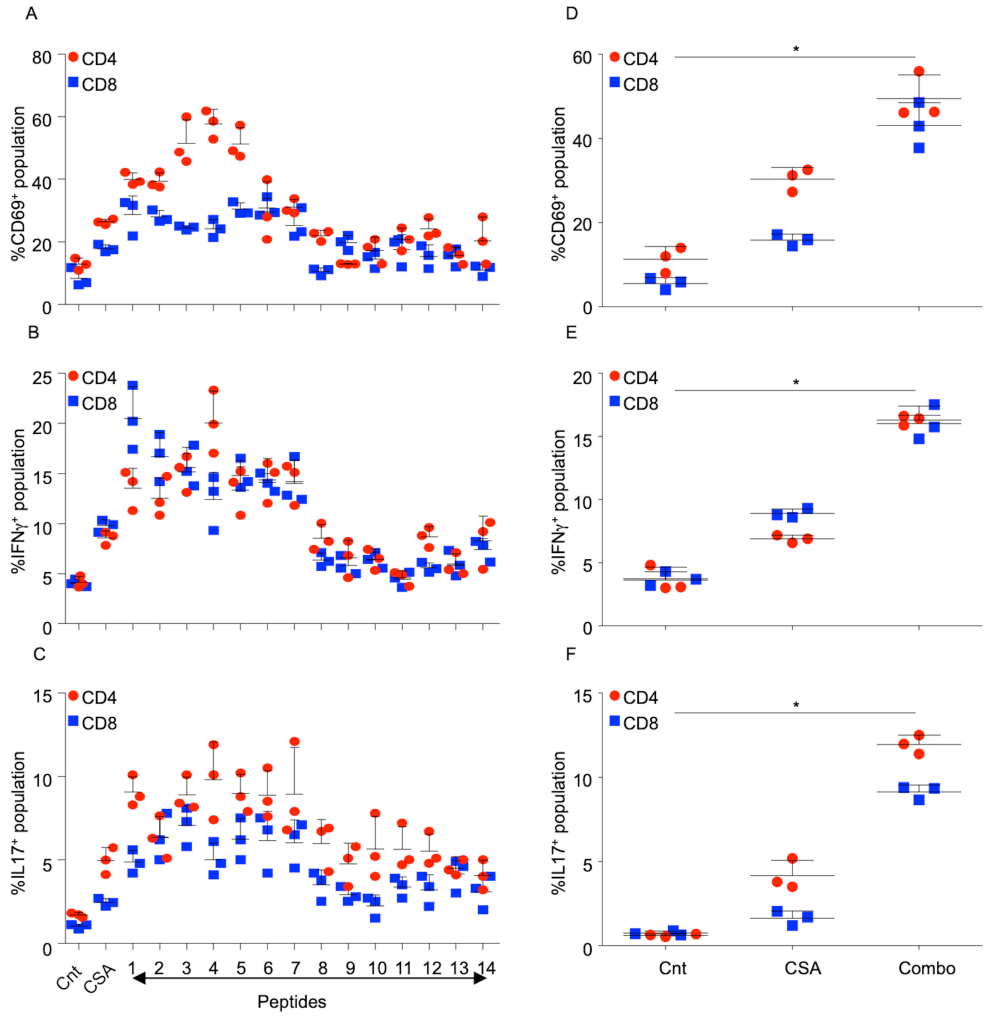

Figure 1: Mycobacterial antigens induce activation of protective T-cells responses. T cells isolated from the spleen of mice infected with H37Rv and treated with DOTS, were stimulated with DCs preloaded with the peptides for 48 h followed by surface-staining with anti-CD3, anti-CD4, anti-CD8, anti-CD69 and staining for intracellular cytokines with anti-IFNγ and anti-IL17 antibodies. Bar graphs depicting the percentage of **(A)** $CD4^+CD69^+$ and $CD8^+CD69^+$ T cells, **(B)** $CD4^+IFN\gamma^+$ and $CD8^+IFN\gamma^+$ T cells, **(C)** $CD4^+IL17^+$ and $CD8^+IL17^+$ T cells. **(D)** Activation of $CD4^+$ and $CD8^+$ T cells co-cultured with unstimulated DCs (Cnt), DCs pulsed with CSA or DCs pulsed with the peptide combo. $CD4^+$ and $CD8^+$ T cells expressing **(E)** IFNγ and **(F)** IL17 after stimulation with the combo. Each experiment was performed at least thrice in triplicates. Two-tailed student's t-test was performed for statistical analysis. Data represents mean ± SD (n=3). *$p<0.05$.

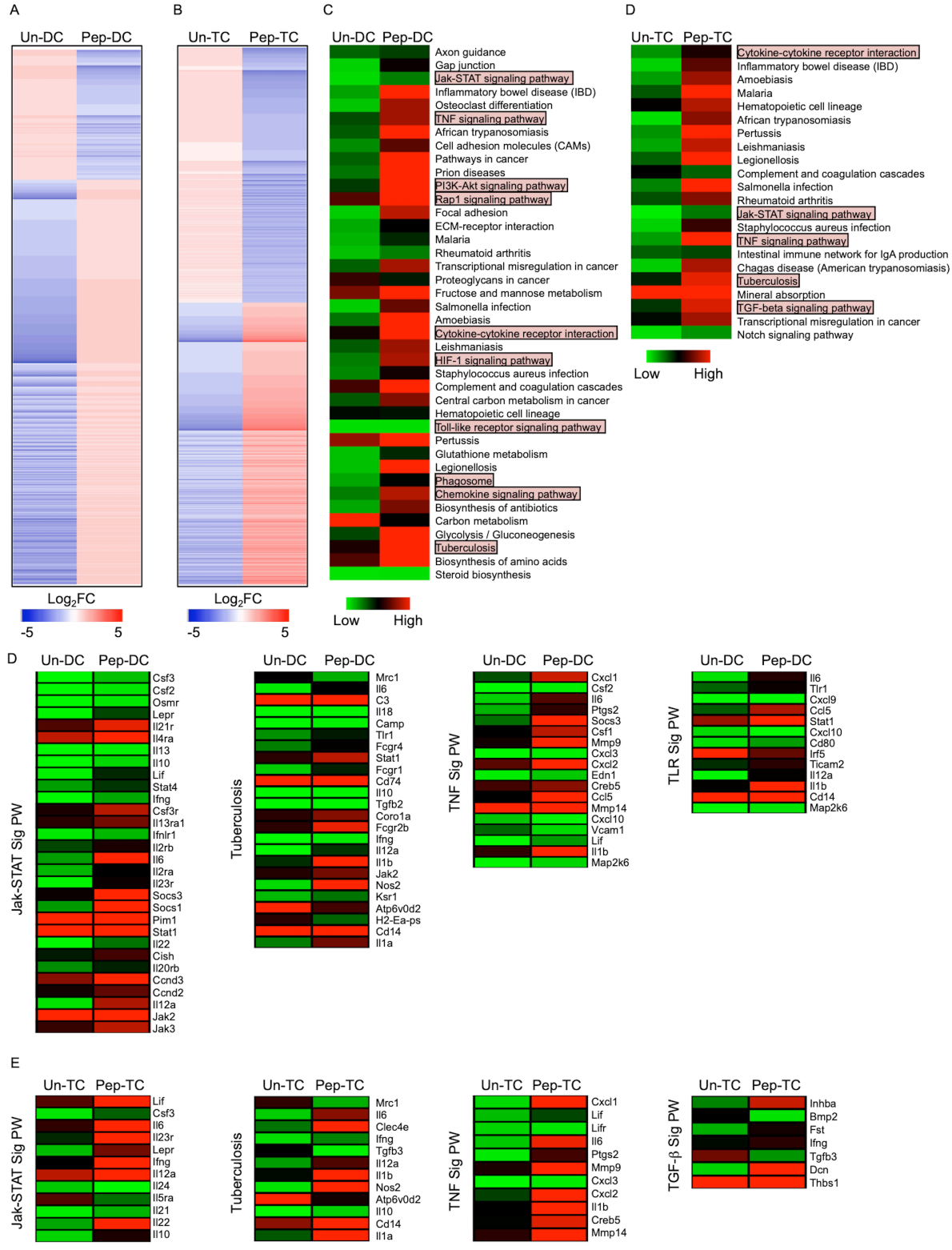

Figure 2: Stimulation with peptide pool induces multiple signaling pathways involved in providing protection during *M.tb* infection. Heatmap representation of the genes differentially expressed in **(A)** the DCs pulsed with peptide pool (Pep-DC) in comparison with unstimulated DCs (Un-DC) and **(B)** the T cells co-cultured with DCs pulsed with peptide pool (Pep-TC) vs T cells co-cultured with unstimulated DCs (Un-TC). Red depicts

activation while blue represents repression. **(C)** Molecular signaling pathways majorly affected in Pep-DCs. **(D)** KEGG pathways significantly modulated in Pep-TCs. **(E)** Heatmaps representing the JAK-STAT signaling pathway, Tuberculosis, TNF signaling pathway and TLR signaling pathways in Pep-DCs vs UN-DCs. **(F)** Heatmaps representing the JAK-STAT signaling pathway, Tuberculosis, TNF signaling pathway and TGFβ signaling pathways in Pep-TCs vs UN-TCs. RNAseq was performed once in triplicates (n=3).

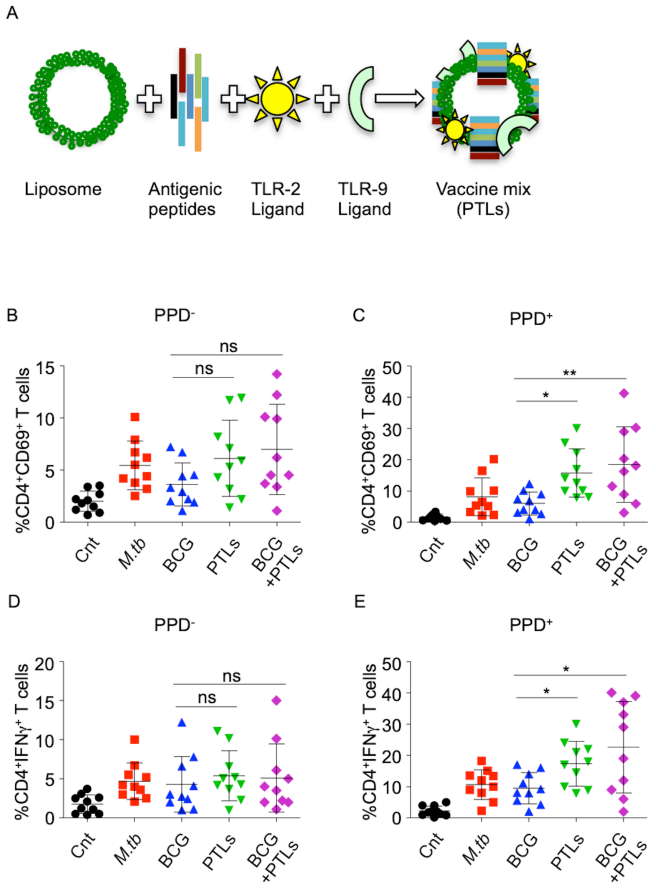

Figure 3: PTLs induce a protective immune response in human PBMCs. (A) Schematic diagram depicts the preparation of PTLs. PBMCs isolated from PPD^- and PPD^+ healthy subjects were *in vitro* stimulated with different mycobacterial antigens for 48h. **(B&C)** Expression of CD69 on $CD4^+$ T cells stimulated with mycobacterial antigens in **(B)** PPD^- and **(C)** PPD^+ individuals. **(D&E)** Percentage of $CD4^+$ T cells expressing IFNγ in the PBMCs of **(D)** PPD^- and **(E)** PPD^+ individuals. One-way ANOVA followed by multiple tukey tests was performed for statistical analysis. Data represents mean±SD (n=10) performed once. *p<0.05, **p<0.005.

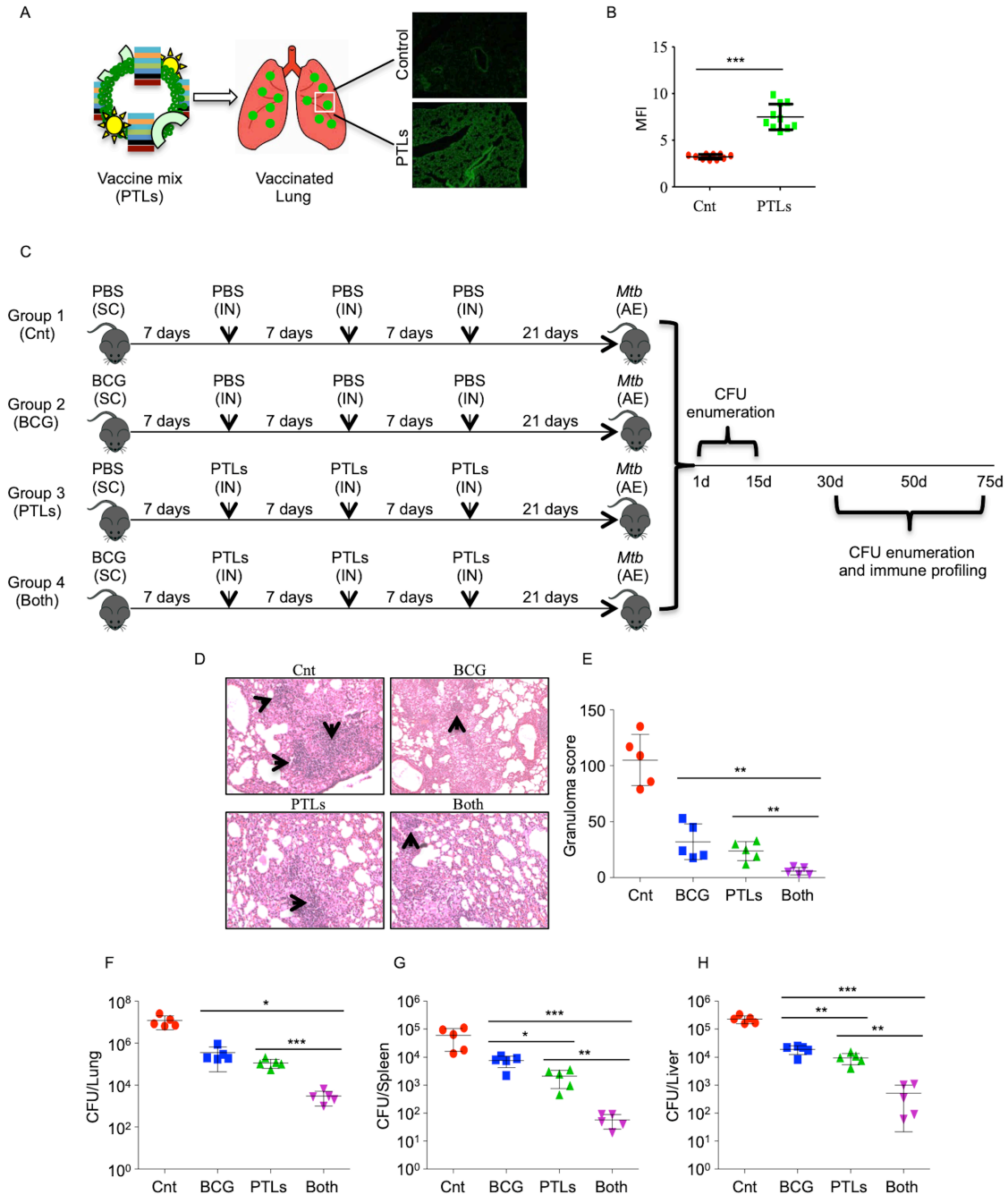

Figure 4: PTLs enhances the efficacy of BCG and protects mice against TB. (A) Lung section to show the accumulation of liposomes. Liposomes were stained with PKH67 dye. **(B)** Quantification of the fluorescent images. **(C)** Layout to show the experimental plan wherein naïve C57BL/6 mice or mice vaccinated with BCG/PTLs or a combination of both were challenged with H37Rv via the aerosol route with a low-dose inoculum of ~150 CFU/mice. Mice were sacrificed at various time points and lungs, spleen and liver were harvested to look at the bacterial burden as well as profiling of immune responses. **(D)** Lungs were harvested, preserved in 4% paraformaldehyde and processed for sectioning and staining with Hematoxylin and Eosin (H&E). **(E)** Quantification of the granuloma (inflammatory lesions) in all experimental groups. **(F)** CFU from the lung, **(G)** spleen and **(H)** liver

homogenates at 50 days post infection. Two-tailed student's t-test was performed for statistical analysis. Data is representative of two independent experiments (n=5 mice/group). *p<0.05, **p<0.005, ***p<0.0005.

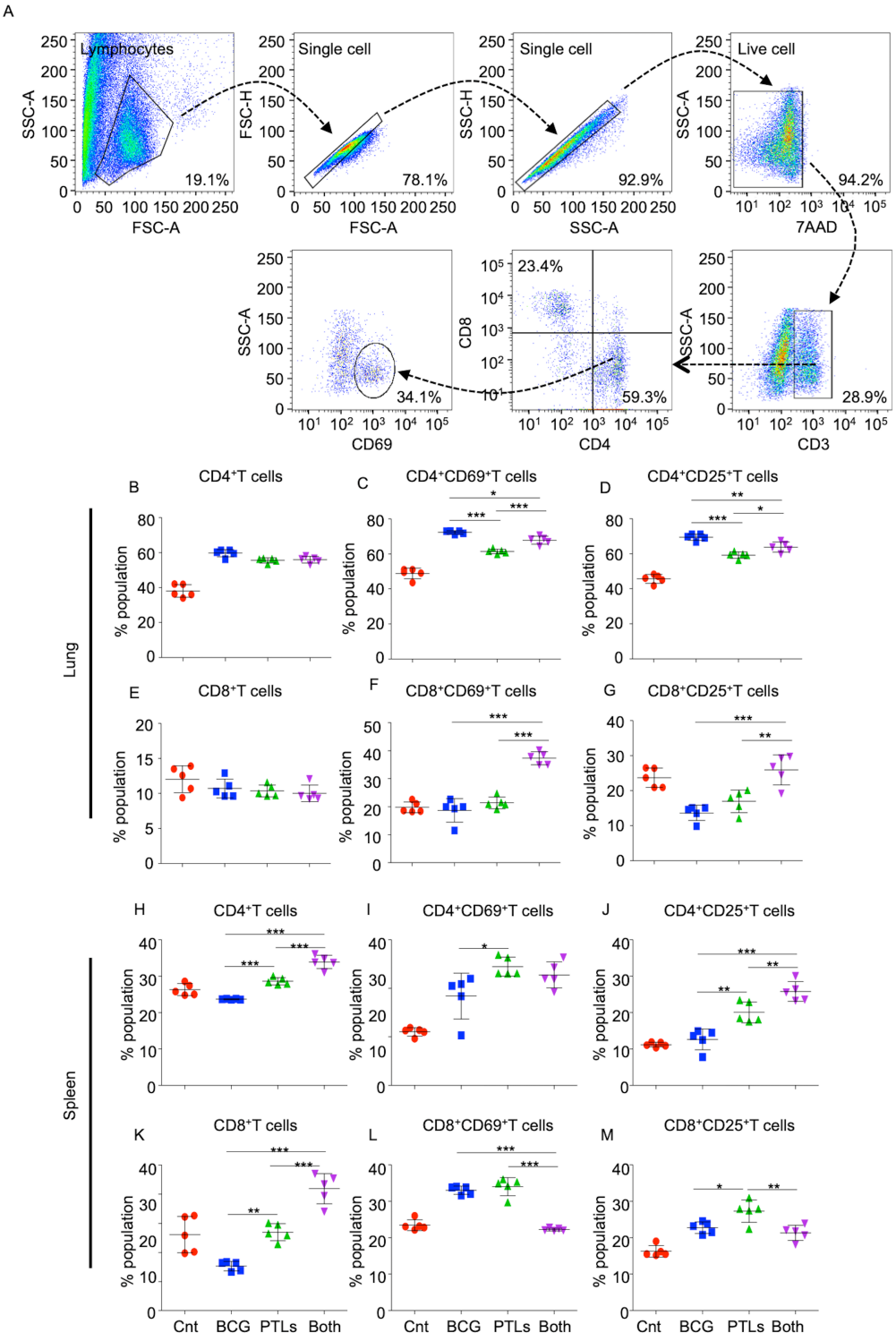

Figure 5: PTLs immunization induces T cell activation in the lungs and the spleen of infected animals. T lymphocytes were isolated from the lungs of all experimental groups and stained with 7AAD, anti-CD3, anti-CD4, anti-CD8, anti-CD25 and anti-CD69 antibodies. **(A)** Gating strategy employed to quantify the T cell activation. **(B)** Percentage of $CD4^+$ T cells and expression of **(C)** CD69 and **(D)** CD25 on $CD4^+$ T cells in the lungs of infected animals. **(E)** Percentage of $CD8^+$ T cells and expression of **(F)** CD69 and **(G)** CD25 on $CD8^+$ T cells in the lungs of infected animals. **(H-M)** T lymphocytes were isolated from the spleen of all

experimental groups and stained with 7AAD, anti-CD3, anti-CD4, anti-CD8, anti-CD25 and anti-CD69 antibodies. Percentage of **(H)** $CD4^+$, **(I)** $CD4^+CD69^+$ and **(J)** $CD4^+CD25^+$ T cells in the spleen of infected animals. Percentage of **(K)** $CD8^+$, **(L)** $CD8^+CD69^+$ and **(M)** $CD8^+CD25^+$ T cells in the spleen of infected animals. One-way ANOVA followed by multiple tukey tests was performed for statistical analysis. Data is representative of two independent experiments (n=5 mice/group). *$p<0.05$, **$p<0.005$, ***$p<0.0005$.

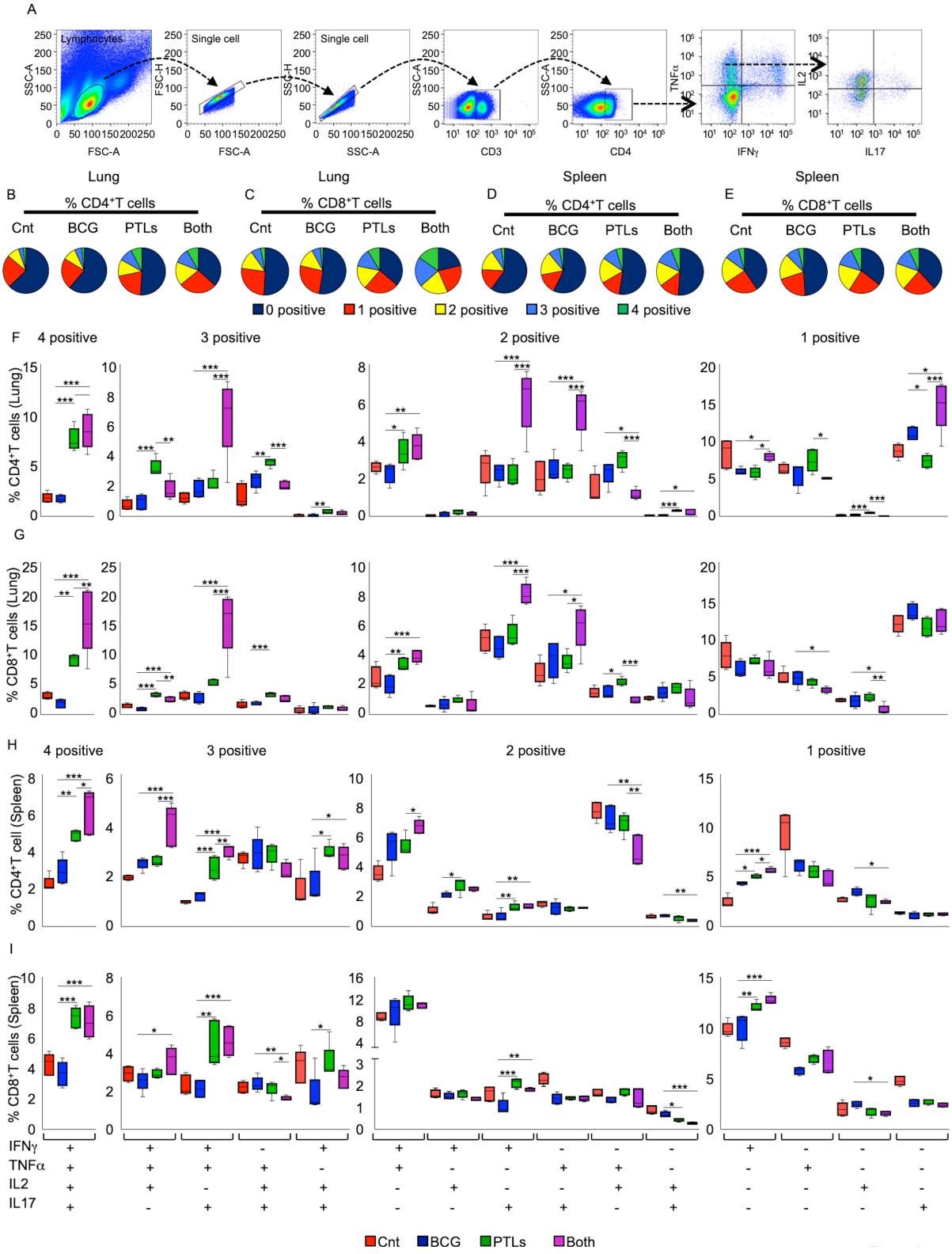

Figure 6: BCG-PTLs co-immunization induces the antigen-specific polyfunctional cytokine responses in the lungs and the spleen of infected animals. (A) Lymphocytes isolated from the lungs of infected animals were stained with anti-CD3, anti-CD4, anti-CD8, anti-IFNγ, anti-TNFα, anti-IL17 and anti-IL2 to assess polyfunctional cytokine responses. Pie charts depicting the percentage of **(B)** $CD4^+$ and **(C)** $CD8^+$ T cells expressing 4, 3, 2, 1 and 0 cytokines (IFNγ, TNFα, IL17 and IL2) in the lungs of the mice. The pie charts

representing the average percentage of cytokine-producing **(D)** $CD4^+$ and **(E)** $CD8^+$ T cells producing five combinations (0^+, 1^+, 2^+, 3^+ and 4^+) of the four cytokines analyzed in the spleen of infected animals. Fifteen possible cytokine combinations are shown for **(F)** $CD4^+$ and **(G)** $CD8^+$ T cells from the lungs of infected animals. Box and whisker plots depicts fifteen combinations of responses for the four cytokines analyzed on the x-axis with the percentage of **(H)** $CD4^+$ and **(I)** $CD8^+$ responding splenic T cells on the y-axis. One-way ANOVA followed by multiple tukey tests was performed for statistical analysis. Data is representative of two independent experiments (n=5 mice/group). *$p<0.05$, **$p<0.005$, ***$p<0.0005$.

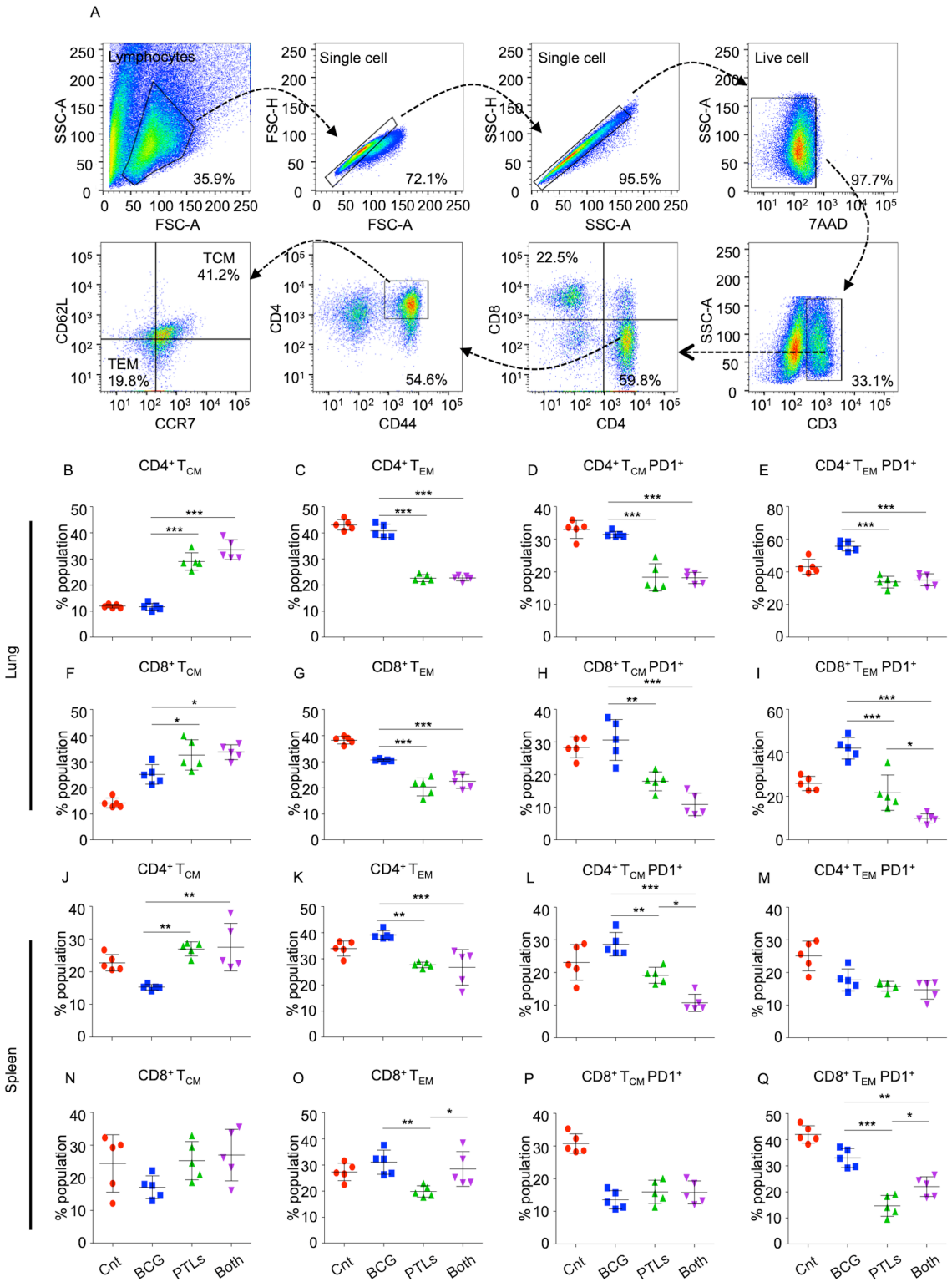

Figure 7: PTLs induces superior antigen specific T-cell memory responses in the lungs and the spleen of infected mice. T lymphocytes isolated from the lungs and the spleen of the indicated groups of experimental mice at 50 days post-infection were surface-stained with anti-CD3, anti-CD4, anti-CD8, anti-CCR7, anti-CD44, anti-CD62L and anti-PD-1 antibodies

and fixed prior to acquisition by flow cytometry. **(A)** Gating strategy employed to quantify the memory T cell responses. Percentage of **(B) c**entral memory (T_{CM}: $CCR7^{HI}CD62L^{HI}CD44^{HI}$) and **(C)** effector memory (T_{EM}: $CCR7^{LO}CD62L^{LO}CD44^{HI}$) $CD4^{+}$ T cells on lymphocytes isolated form the lungs of infected animals. Frequency of PD-1 expression on **(D)** central memory and **(E)** effector memory $CD4^{+}$ T cell subset. Percentage of **(F) c**entral memory (T_{CM}: $CCR7^{HI}CD62L^{HI}CD44^{HI}$) and **(G)** effector memory (T_{EM}: $CCR7^{LO}CD62L^{LO}CD44^{HI}$) $CD8^{+}$ T cells on lymphocytes isolated form the lungs of infected animals. **(H&I)** Frequency of PD-1 expression on these cell subsets. **(J-Q)** Frequency of **c**entral memory, effector memory, and PD-1 expression on these cell subsets on the lymphocytes isolated form the spleen of infected mice. One-way ANOVA followed by multiple tukey tests was performed for statistical analysis. Data is representative of two independent experiments (n=5 mice/group). *$p<0.05$, **$p<0.005$, ***$p<0.0005$.

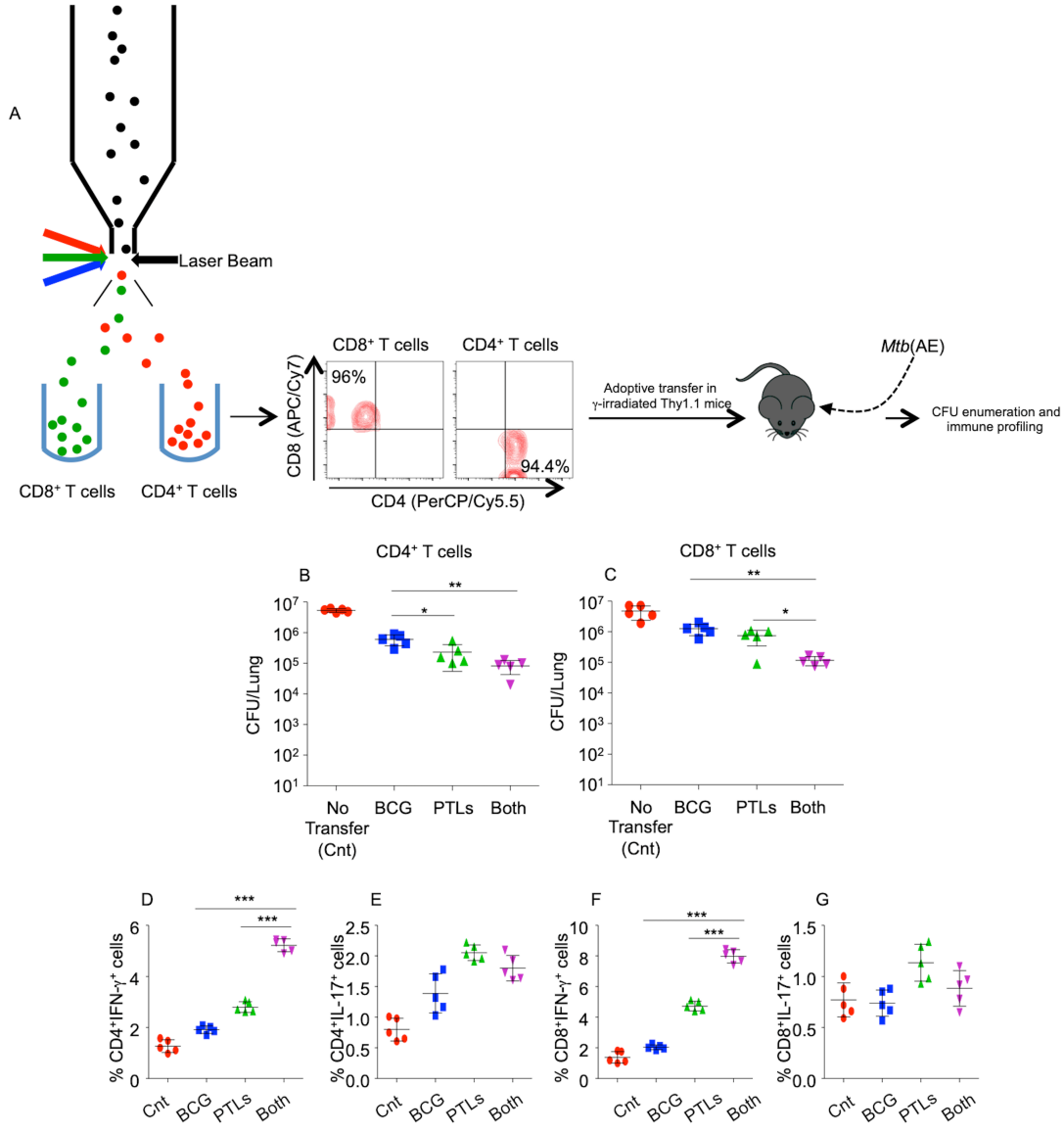

Figure 8: T cells from BCG-PTLs co-immunized mice confer improved protection against TB. (A) T lymphocytes isolated from BCG, PTLs or BCG-PTLs immunized and *M.tb* infected animals (50 days post infection) were subjected to surface staining with anti-CD3, anti-CD4 and anti-CD8 followed by sorting by FACS Aria into two distinct populations: $CD4^+$ and $CD8^+$ T cells. Sorted $CD4^+$ and $CD8^+$ T cells were cultured overnight and transferred into irradiated recipient Thy1.1 mice. Seven days after adoptive transfer, all mice were challenged with *M.tb* H37Rv through the aerosol route. At 25 days post infection, the mice were euthanized for CFU enumeration and immune profiling. CFU in the lungs of mice receiving **(B)** $CD4^+$ and **(C)** $CD8^+$ T cells. **(D-G)** Dot plots representing the percentage of INFγ and IL17 producing $CD4^+$ and $CD8^+$ T cells in the spleen of infected mice. Two-tailed student's t-test was performed for statistical analysis in **B** and **C**. One-way ANOVA followed by multiple tukey tests was performed for statistical analysis for **D-G**. Data is representative of two independent experiments (n=5 mice/group). *p<0.05, **p<0.005.

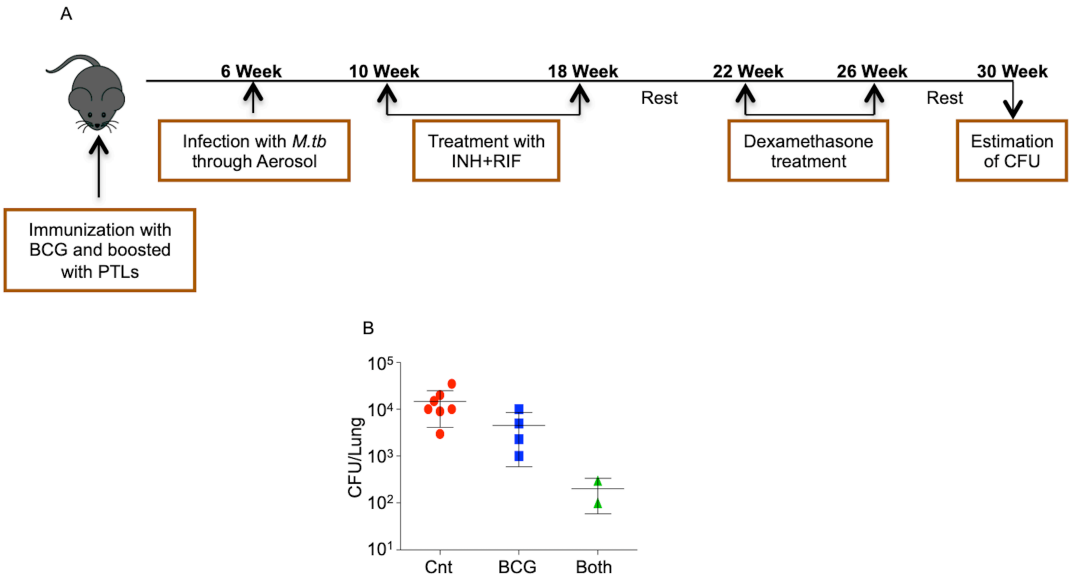

Figure 9: PTLs immunization reduces the recurrence of DOTS associated disease relapse. (A) Mice co-immunized with PTLs and BCG were infected with H37Rv *M.tb* followed by treatment with isoniazid and rifampicin for 16 weeks. After 30 days of rest, these mice were treated with dexamethasone for 30 days followed by one more period of rest for 30 days. Mice were then sacrificed for CFU estimation to determine the rate of relapse post-treatment. **(B)** CFU from the lung homogenates of the mice. The reactivation experiment was done once with 10 mice in each group.

Table 1: Determination of reactivation rate of latent *M.tb*

Group	Reactivation rate*
Control	7/10
BCG immunized	4/9
BCG immunized and boosted with mimic	2/10

*Number of mice re-activated out of total number of mice in that group.

Supplementary Figures and Legends:

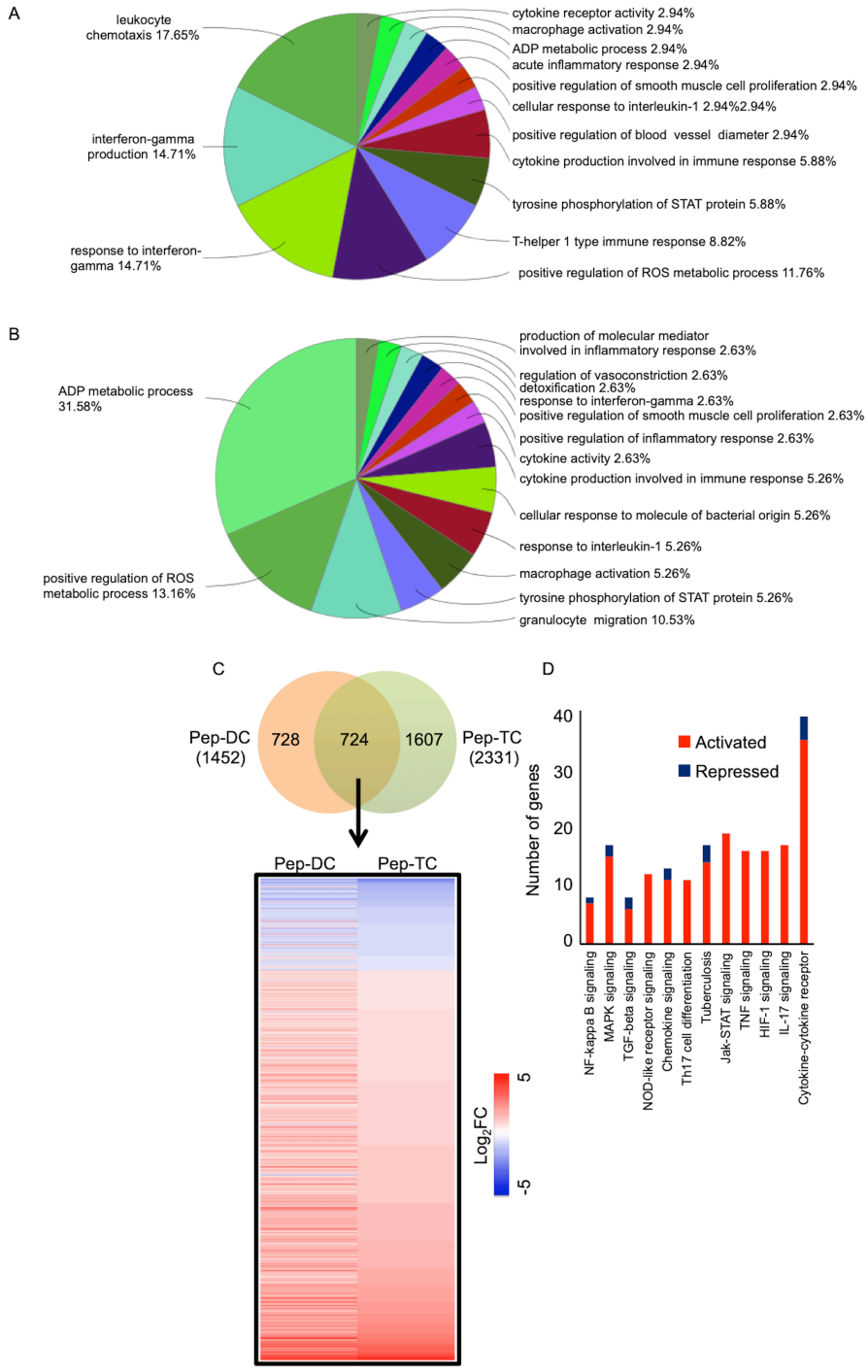

Supplementary Figure 1: *M.tb* peptides induce upregulation of genes that confer protection against TB in both DCs and T cells. (A) Pie diagram indicating the GO biological processes upregulated in DCs pulsed with peptide pool as compared to unstimulated DCs. **(B)** Pie chart indicating the percentage of genes belonging to different GO biological processes in stimulated T cells as compared to unstimulated T cells. **(C)** Heatmap depicting the expression profile of the genes common between the DCs and T cells. **(D)** KEGG pathway analysis of the shared genes representing the significantly affected pathways. **Un-DC**: unstimulated DCs, **Pep-DC**: DCs pulsed with peptide pool, **Un-TC**: T cells co-

cultured with unstimulated DCs, **Pep-TC**: T cells co-cultured with DCs pulsed with peptide pool. RNAseq was performed once in triplicates (n=3).

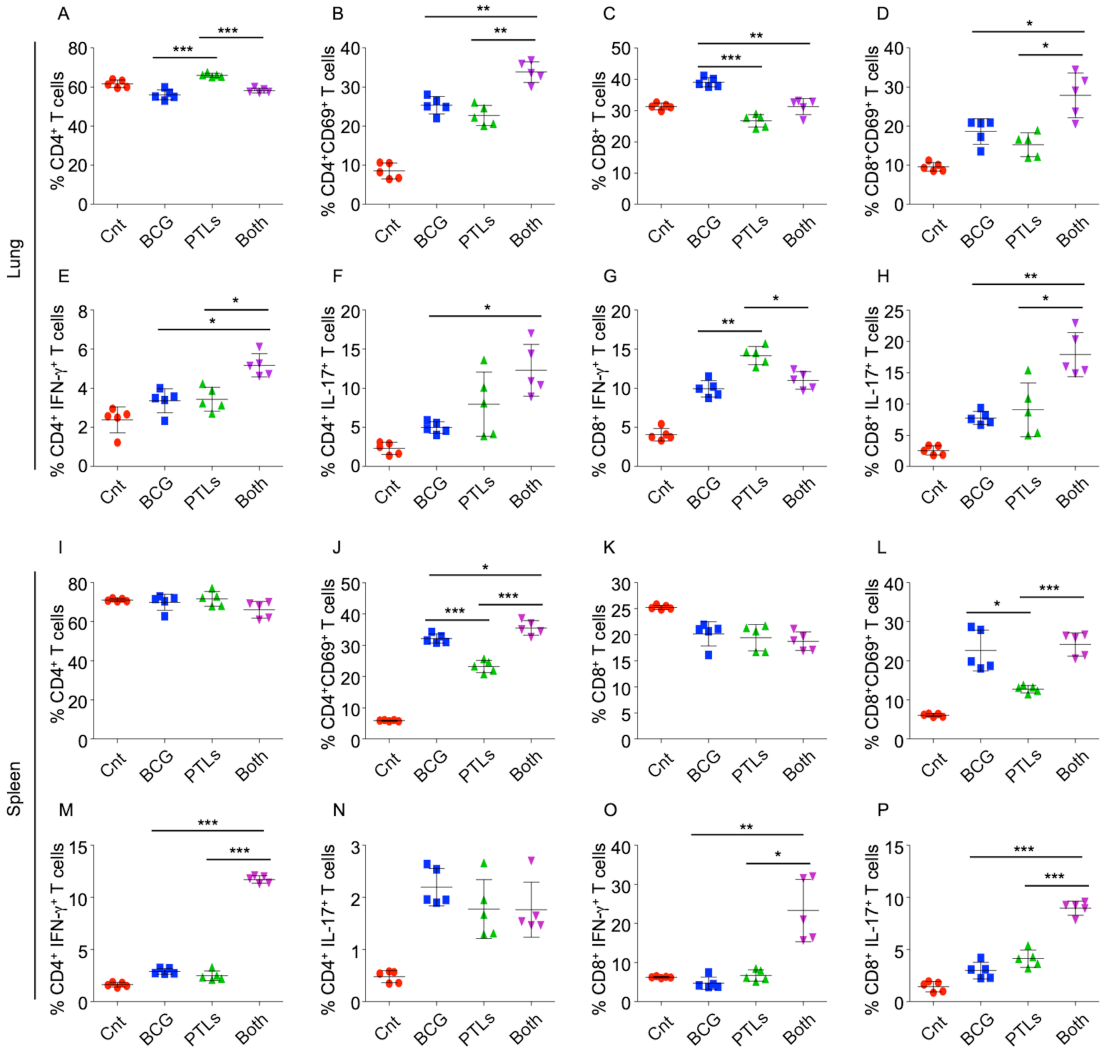

Supplementary Figure 2: Pre-challenge immune responses in the lungs and the spleen of vaccinated mice. (A-H) T lymphocytes were isolated from the lungs of all experimental groups and stained with 7AAD, anti-CD3, anti-CD4, anti-CD8, anti-CD69, anti-IFNγ and anti-IL17 antibodies. Percentage of $CD4^+$ T cells **(A),** $CD4^+CD69^+$ T cells **(B)**, $CD8^+$ T cells **(C)** and $CD8^+CD69^+$ T cells **(D)** in the lungs of unvaccinated (Cnt) and vaccinated animals. **(E-H)** Expression of IFNγ and IL17 on $CD4^+$ and $CD8^+$ T cells in the lungs. **(I-P)** T lymphocytes isolated from the spleen of all experimental groups were stained with 7AAD, anti-CD3, anti-CD4, anti-CD8, anti-CD69, anti-IFNγ and anti-IL17 antibodies. Percentage of $CD4^+$ T cells **(I),** $CD4^+CD69^+$ T cells **(J)**, $CD8^+$ T cells **(K)** and $CD8^+CD69^+$ T cells **(L)** in the spleen of different groups. **(M-P)** Expression of IFNγ and IL17 on $CD4^+$ and $CD8^+$ T cells in the spleen. One-way ANOVA followed by multiple tukey tests was performed for statistical analysis. Data is representative of two independent experiments (n=5 mice/group). *p<0.05, **p<0.005, ***p<0.0005.

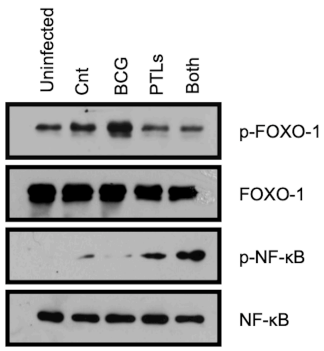

Supplementary Figure 3: Enhanced NFkB and FOXO1 activation in the spleen of infected mice co-immunized with BCG-PTLs. Cell lysates prepared from the splenocytes of infected mice from all the experimental groups were used to analyze the phosphorylation status of FOXO1 and NFkB by immunoblotting. Data is representative of two independent experiments.

Supplementary Table 1: List of Peptides used in the study

S. No.	Peptide Sequence	Position	Protein name	Rv number
P1	AWGRRLMIGTAAAVVLPG	10aa - 27aa	Ag85B	Rv1886c
P2	TAAAVVLPGLVGLAGGAA	19aa - 36 aa	Ag85B	Rv1886c
P3	WDINTPAFEWYYQSGLSI	91aa - 108aa	Ag85B	Rv1886c
P4	LDEGKQSLTKLAAAW	29aa - 43aa	ESAT6	Rv3875
P5	KQSLTKLAAAWGGSG	33aa - 47aa	ESAT6	Rv3875
P6	TKLAAAWGGSGSEAY	37aa - 51aa	ESAT6	Rv3875
P7	LARTISEAGQAMASTEGNVTGMFA	72aa - 95aa	ESAT6	Rv3875
P8	AVAASNNPELTTLTAALSGQLNPQV	61aa-85aa	Mpt70	Rv2875
P9	ALSGQLNPQVNLVDTLNSGQYTVFA	76aa-100aa	Mpt70	Rv2875
P10	FSKLPASTIDELKTNSSLLTSILTY	106aa-130aa	Mpt70	Rv2875
P11	GNADVVCGGVSTANATVYMIDSVLM	166aa-190aa	Mpt70	Rv2875
P12	TVYMIDSVLMPPA	181aa-193aa	Mpt70	Rv2875
P13	AVDAADKVLGYRNWL	278-292aa	GlcB	Rv1837
P14	KVLGYRNWLGLNKGD	284-298aa	GlcB	Rv1837

Supplementary Table 2: List of seven antigenic peptides used for further studies. Experiments from A-C were repeated with the pool of seven peptides.

Peptides	Sequences
P-1	AWGRRLMIGTAAAVVLPG
P-2	TAAVVLPGLVGLAGGAA
P-3	WDINTPAFEWYYQSGLSI
P-4	KQSLTKLAAAWGGSG
P-5	TKLAAAWGGSGSEAY
P-6	LDEGKQSLTKLAAAW
P-7	LARTISEAGQAMASTEGNVTGMEA